HOKKAIDO UNIVERSITY

Title	Epigenetic patterns at the mouse prolyl oligopeptidase gene locus suggest the CpG island in the gene body to be a novel regulator for gene expression
Author(s)	Matsubara, Shin; Takahashi, Takayuki; Kimura, Atsushi P.
Citation	GENE, 465(1-2), 17-29 https://doi.org/10.1016/j.gene.2010.06.006
Issue Date	2010-10-01
Doc URL	http://hdl.handle.net/2115/43940
Type	article (author version)
File Information	Matsubara-Gene2010re.pdf

Instructions for use

Hokkaido University Collection of Scholarly and Academic Papers : HUSCAP

Epigenetic patterns at the mouse prolyl oligopeptidase gene locus suggest the CpG island in the gene body to be a novel regulator for gene expression.

Shin Matsubara[a], Takayuki Takahashi[ab], and Atsushi P. Kimura[ab]*

[a]Graduate School of Life Science, [b]Department of Biological Sciences, Faculty of Science, Hokkaido University, Sapporo 060-0810, Japan

Running title: Epigenetic regulation of the mouse *POP* gene

*Corresponding author: Atsushi P. Kimura, Laboratories of Functional Biology, Department of Biological Sciences, Faculty of Science, Hokkaido University, Sapporo 060-0810, Japan. Phone and Fax: 81-11-706-4452. E-mail: akimura@sci.hokudai.ac.jp

Disclosure summary: The authors certify that they have nothing to disclose.

Abstract

Prolyl oligopeptidase (POP) is a widely distributed serine peptidase which hydrolyzes small peptides on the carboxyl side of an internal proline residue. While its physiological role has been intensely studied, the regulatory mechanism of the gene expression is poorly understood. This time we assessed the *POP* mRNA expression in mouse embryos and tissues related to reproduction and development and found that *POP* mRNA was highly expressed in the ovarian granulosa cell, placental spongiotrophoblast, and blastocyst embryo. To elucidate the mechanism by which *POP* expression is regulated, we investigated DNA methylation and histone modification patterns of the two CpG islands (CGIs) found at the mouse *POP* locus. Whereas the CGI including the *POP* promoter (CGI-1) was completely hypomethylated in all the tissues examined, DNA methylation level of the CGI in the gene body (CGI-2) was lower in the granulosa cell, placenta, and blastocyst than in the liver. Some specific CpGs in CGI-2 were significantly demethylated in the three tissues. An *in vitro* reporter analysis indicated that CGI-2 enhanced *POP* promoter activity and its effect was significantly reduced by DNA methylation. Moreover, histone H3 acetylation and H3K4 methylation levels of CGI-2 were higher in the granulosa cell than liver. The results suggest that the CGI-2 region is a *cis*-element for the *POP* gene expression.

Key words: prolyl oligopeptidase, granulosa cell, blastocyst, DNA methylation, histone acetylation, histone H3K4 methylation

Abbreviations: BCIP, 5-bromo-4-chloro-3-indolyl phosphate; CGI, CpG island; ChIP, chromatin immunoprecipitation; CIAA, chloroform-isoamylalcohol; DIG, digoxigenin; DMEM, Dulbecco's modified Eagle's medium; FBS, fetal bovine serum ; hCG, human chorionic gonadotropin; ICR, imprinting control region; NBT, nitroblue tetrazolium; PBS, phosphate-buffered saline; POP, prolyl oligopeptidase; RT-PCR, reverse transcription-polymerase chain reaction; SD, standard deviation

1. Introduction

Prolyl oligopeptidase (POP, E.C.3.4.21.26, also known as prolyl endopeptidase and post-proline cleaving enzyme; gene symbol *Prep*) is a widely distributed serine endopeptidase which selectively digests -Pro-X- bonds of peptides (Wilk, 1983). Since its discovery in the human uterus as an oxytocin-inactivating enzyme (Walter et al., 1971), much effort has been focused on understanding its physiological role as reviewed elsewhere (Garcia-Horsman et al., 2007; Myöhänen et al., 2009; Williams 2004). POP-deficient mice have been very recently reported and the results demonstrated that the mice had a defect in growth cone dynamics of neurons (Di Daniel et al., 2009) and exhibited a parent of origin effect on obesity due to an inability to process α-melanocyte stimulating hormone (Perroud et al., 2009; Warden et al., 2009). While these studies have improved our knowledge about its role, the regulatory mechanism of the gene expression remains to be elucidated. It is well known that POP is distributed differently among tissues and between various regions in the brain (Agirregoitia et al., 2003; Bellemere et al., 2004; Goossens et al., 1996; Irazusta et al., 2002; Myöhänen et al., 2007, 2008a, 2008b, 2009; Schulz et al., 2005). In addition, the expression was disturbed in the brain of patients of neurodegenerative diseases and increased in some cancerous cells (Garcia-Horsman et al., 2007; Goossens et al., 1996; Williams, 2004). These suggest that the *POP* gene is highly regulated in each tissue and therefore it is of great importance to clarify the mechanism controlling the *POP* gene.

Epigenetic control of chromatin structure is essential for eukaryotic gene activation and inactivation and this regulation is mainly performed by DNA methylation and histone modification. In mammals the cytosine of a CpG dinucleotide can be methylated and any gene whose promoter is highly methylated is silenced. Generally, a housekeeping gene has the GC-rich promoter which is hypomethylated and thereby the gene is actively transcribed (Caiafa

and Zampieri, 2005). Genes expressed in a tissue-specific manner do not always have GC-rich promoters and instead are often regulated by a CpG island (CGI) located far from the promoter (Illingworth and Bird, 2009). This indicates that in mammals, CpG methylation of promoters or other control regions plays an important role in the regulation of many genes. The other epigenetic status is the post-translational modification of core histone proteins such as acetylation, methylation, and phosphorylation, and the modification pattern defines the chromatin structure. For example, histone H3 and H4 acetylation and H3K4 methylation are associated with open chromatin leading to gene activation (Berger, 2002; Choi and Howe, 2009; Hublitz et al., 2009). Histone H3K9 and H3K27 methylation contribute to the formation of tightly packaged chromatin resulting in gene silencing (Hublitz et al., 2009; Martin and Zhang, 2005). Thus, the histone modification pattern is crucial for controlling gene expression. The DNA methylation and histone modification are functionally linked with each other to regulate gene expression (Cedar and Bergman, 2009; Ng and Bird, 1999).

The mouse *POP* gene, located on chromosome 10B2, is about 92 kb long containing 15 exons, and the neighboring genes are positioned more than 130 kb away (Fig. 1). Although our previous results showed that a 200-bp 5' flanking sequence is sufficient for *in vitro* activation of a reporter gene (Kimura et al., 1999), it is not known how the gene is epigenetically controlled or if there are other sequences to control its expression. In this study, we examined *POP* mRNA expression in mouse tissues related to reproduction and development and found that the ovarian granulosa cell, placental spongiotrophoblast, and blastocyst embryo expressed a high level of *POP* mRNA. To investigate the regulatory mechanism for the *POP* gene, we analyzed the CpG methylation and histone modification of two CGIs (CGI-1 and CGI-2) found at the *POP* gene locus. The results suggest that CGI-2 plays a role in the regulation of *POP* expression.

2. Materials and Methods

2.1. *Animals*

The mice (C57/BL6) were maintained at 25°C with a photoperiod of 14:10 h light: dark with free access to food and water. Embryonic day (E) was determined based on the day we checked the vaginal plug and the embryos' characteristics. The experimental procedures used in this study were approved by the Institutional Animal Use and Care Committee at Hokkaido University.

2.2. *reverse transcription-polymerase chain reaction (RT-PCR) analysis*

Total RNA was purified from each tissue using Isogen (Nippon gene, Tokyo, Japan) according to the manufacturer's instructions and the first-strand cDNA was synthesized using a Superscript III reverse transcriptase (Invitrogen, Carlsbad, USA). The primers for *POP* (Fig. 1), *GAPDH* (Kwon et al., 2006), *β-actin* (Fraczek et al., 2008), and *aryl-hydrocarbon receptor-interacting protein (Aip)* are shown in Table 1. Quantitative RT-PCR (qRT-PCR) was performed using the 7300 real-time PCR system and Power SYBR Green PCR Master Mix (Applied Biosystems, Foster City, USA) in a total volume of 10 μl per well. The amplification conditions were 50°C for 2 min, 95°C for 10 min, and 40 cycles of 95°C for 15 sec and 60°C for 30 sec. Dissociation curves were obtained to confirm the specificity of the amplified DNA. The data were separately normalized with *GAPDH*, *β-actin*, and *Aip*.

To investigate the expression of genes surrounding *POP*, RT-PCR analysis was performed with ExTaq DNA polymerase (Takara, Ohtsu, Japan) in a total volume of 5 μl. The primers for *Atg5*, *Prdm1*, *Popdc3*, *Bves*, *Lin28b*, and *Hace1* are listed in Table 2. The PCR conditions were 94°C for 3 min, and 30 cycles of 94°C for 15 sec, 60°C for 30 sec, and 72°C for 30 sec. The amplified products were evaluated by agarose gel electrophoresis and ethidium bromide staining.

The expression of the *Atg5* and *Hace1* genes was also assessed by qRT-PCR using the same primers as used above (Table 2).

2.3. *In situ hybridization*

Probes were obtained by RT-PCR with mouse placental total RNA using primer pairs for *POP* and *Flt1* (Hitz et al., 2005). The position of the *POP* probe is depicted in Fig. 1 and the primer sequences are shown in Table 1. Sense and antisense cRNA probes were synthesized by *in vitro* transcription using digoxigenin (DIG)-UTP (Roche Molecular Biochemicals, Mannheim, Germany) and T3 or T7 RNA polymerase (Promega Corporation, Madison, USA).

Placentas at E17.5 and ovaries from superovulated mice were slowly frozen in tissue-tek (Sakura Finetek USA, Inc., Torrance, USA) and kept at -80°C until use. The sections (10 μm) were cut on a cryostat and thaw-mounted onto MAS-coated slides. The sections were fixed with 4% paraformaldehyde (Wako Pure Chemicals, Osaka, Japan) in phosphate-buffered saline (PBS) for 10 min and washed with PBS for 5 min three times. The sections were treated with 1 μg/ml proteinase K (Roche Molecular Biochemicals) for 2-3 min at room temperature and refixed in the same fixative for 10 min. The slides were washed again with PBS and acetylated with 0.25% acetic anhydride in 0.1 M triethanolamine/HCl (Sigma, St. Louis, USA), pH 8.0 for 10 min. After prehybridization for 2-3 h at room temperature in 50% formamide (Roche Molecular Biochemicals), 6×SSPE (0.15 M NaCl, 8.65 mM NaH_2PO_4, 1.25 mM EDTA, pH 7.4), 5×Denhardt's solution (Wako Pure Chemicals), and 500 μg/ml yeast transfer RNA (Roche Molecular Biochemicals), the sections were incubated at 60°C for 16-18 h in the same buffer containing 100-200 ng/ml DIG-labeled cRNA probes. The hybridized sections were washed three times in 0.2×SSC at 60°C for 20 min. The slides were incubated in 1% blocking reagent (Roche Molecular Biochemicals) in DIG buffer 1 (100 mM maleic acid, 150 mM NaCl, pH 7.5) for 2-3 h and then in 1:5,000 diluted anti-DIG antibody in DIG buffer 1 containing 1% blocking

reagent for 30 min. After being washed twice with DIG buffer 1 for 15 min and equilibrated with freshly prepared DIG buffer 3 (100 mM Tris-HCl, 100 mM NaCl, 50 mM $MgCl_2$, pH 9.5) for 5 min, the sections were incubated at room temperature with nitroblue tetrazolium /5-bromo-4-chloro-3-indolyl phosphate (NBT/BCIP) in DIG buffer 3 for 16-18 h.

2.4. *Primary granulosa cell culture*

To induce superovulation, female mice (4-5 weeks) were injected with 5IU of pregnant mare serum gonadotropin (PMSG; Sigma) followed 48 hr later by 5IU of human chorionic gonadotropin (hCG; Wako Pure Chemicals). The mice were sacrificed at 5 h after hCG injection and preantral follicles were punctured in Dulbecco's modified Eagle's medium (DMEM) /F12 medium containing 10% fetal bovine serum (FBS) with a 26G needle. After being washed three times with the same medium, the cells were spread on fibronectin-coated dishes and cultured at 37°C under 5% CO_2 in air.

2.5. *In vitro fertilization*

In vitro fertilization was conducted as previously described (Nagy et al., 2002). Preimplantation embryos were obtained at 24, 48, and 96 h after fertilization each corresponding to 2-cell, 3-4 cell, and blastocyst stage embryos. Unfertilized eggs were collected after removing cumulus cells by brief exposure to HTF medium containing 0.3 mg/ml hyaluronidase (Wako Pure Chemicals).

2.6. *Northern blot analysis*

Total RNA was isolated as above. Twenty micrograms of the RNA were electrophoresed on a formaldehyde/agarose gel and transferred to a Hybond-N^+ membrane (GE Healthcare, Piscataway, USA). The blot was hybridized for 16-18 h with a ^{32}P-labeled 262-bp

*Hin*dIII-*Bam*HI fragment of mouse *POP* cDNA (Fig. 1) at 42°C in 50% formamide, 5×Denhardt's solution, 5×SSPE, 1% SDS, and 100 μg/ml herring sperm DNA. The membrane was washed twice at room temperature in 2×SSC/0.05% SDS for 5 min, three times at 50°C in the same buffer for 30 min, and three times at 50°C in 0.1×SSC/0.1% SDS for 30 min, and exposed to Kodak Biomax film (Kodak, Rochester, USA). The signals were visualized by autoradiography. The probe for *GAPDH* was prepared by RT-PCR (Takano et al., 2004) and used as an internal control.

2.7. *Bisulfite sequencing analysis*

Genomic DNA was extracted from each tissue by incubation in digestion buffer (50 mM Tris-HCl, pH 7.5 20 mM EDTA, 100 mM NaCl, 0.5% SDS, 0.2 mg/ml proteinase K) for 16 h at 50°C and extraction with phenol/chloroform-isoamylalcohol (CIAA). The DNAs (0.1-3 μg) were digested with 10 μg/ml RNase A and *Eco*RI at 37°C for 20 h and purified by phenol/CIAA extraction and ethanol precipitation. The digested DNAs were then denatured with 0.3 M NaOH at 37°C for 15 min and mixed with freshly prepared sodium bisulfite (pH 5.0) and hydroquinone at a final concentration of 4.0 M and 0.5 mM, respectively. The mixtures were incubated with a thermal cycler for 15 cycles of 95°C for 30 sec and 50°C for 15 min. After being purified with a Wizard DNA Clean-Up System (Promega), the DNA was treated with 0.3 M NaOH at 37°C for 15 min and purified by ethanol precipitation.

We searched for CGIs at the mouse *POP* locus using the CpG Island Searcher (http://cpgislands.usc.edu/) with the following parameters: minimum length 500 bp, GC content greater than 55%, and ratio CpG observed/expected greater than 0.65. As a result we found two CGIs, CGI-1 and CGI-2 (Fig. 1). CGI-1 is 1344 bp long, spanning the promoter and exon 1 regions. CGI-2 is 614 bp, partially overlapping with exon 15. PCR was performed with ExTaq DNA polymerase (Takara) using the primers listed in Table 1. The reaction conditions for CGI-1

were 94°C for 3 min, 10 cycles of 94°C for 30 sec, 65°C (-1°C /cycle) for 30 sec, and 72°C for 2 min, followed by 30 cycles of 94°C for 30 sec, 55°C for 30 sec, and 72°C for 2 min. For CGI-2 the conditions were 94°C for 3 min, then 40 cycles of 94°C for 30 sec, 58°C for 30 sec, and 72°C for 2 min. Nested PCR was performed for the blastocyst sample using the internal primers for CGI-1 and CGI-2. The profile of the second PCR for CGI-1 was 94°C for 3 min, and 40 cycles of 94°C for 30 sec, 57°C for 30 sec, and 72°C for 2 min. That of the first and second PCRs for CGI-2 was 94°C for 3 min, and 30 and 40 cycles of 94°C for 30 sec, 58°C for 30 sec, and 72°C 1 min, respectively. The amplified products were subcloned into a pBluescript vector (Stratagene, La Jolla, USA) by the TA-cloning method, and 10 subclones for each tissue sample and 20 subclones for the blastocyst were sequenced.

2.8. *Reporter constructs*

A 914-bp *Eco*RI-*Bam*HI fragment of the 5'-flanking sequence of the mouse *POP* gene (Fig. 1) was inserted upstream of the luciferase gene of pGL3-Basic (Promega). After its *Mlu*I site was destroyed, the CGI-2 sequence was inserted downstream of the luciferase gene. The CGI-2 sequence was amplified by PCR with mouse genomic DNA and KOD-plus DNA polymerase (Toyobo, Osaka, Japan) using 5'-AT<u>ACGCGT</u>AGTGGTGGCCTAAATGATGG-3' and 5'-ACCAACCCAAAACATCAAGG-3'. The underlined region indicates the *Mlu*I site. The sequence and the direction of the inserted DNA fragments were confirmed by DNA sequencing method.

For generating the constructs with hypermethylated CGI-2, 50 μg of the plasmid was digested with *Mlu*I and *Sal*I to cut out the CGI-2 region. The vector and CGI-2 fragments were purified separately and collected in 40 μl TE. The CGI-2 fragment was then subjected to CpG methylation by *Sss*I (New England Biolab, Ipswich, USA). For 100% methylation, 2.5 μl of the DNA was treated with 10U of *Sss*I at 37°C for 4 h and for 50% methylation 1U of *Sss*I was used

at 37°C for 30 min. The DNA methylation state was confirmed by *Hha*I digestion and bisulfite sequencing. The methylated or unmethylated CGI-2 fragments were then ligated with a kit (Takara) at 16°C for 16 h to their original vectors. After digestion with *Sal*I at 37°C for 2-3 h, the appropriate length of DNA fragment was purified by Geanclean kit (Qbiogene, Vista, USA). The quantity of each construct was evaluated by agarose gel electrophoresis.

2.9. *Cell culture, reporter gene transfection, and luciferase activity assay*

The cell lines, Hepa1-6 (RCB1638) and NIH3T3-3-4 (RCB1862), were obtained from RIKEN Cell Bank (Tsukuba, Japan) and cultured in DMEM containing 10% FBS, 100 U/ml penicillin, 100 μg/ml streptomycin, and 292 μg/ml L-glutamine (Invitrogen). Transfection was performed in 24-well plates using Lipofectamine 2000 (Invitrogen) according to directions. Luciferase activity was measured 48 h after transfection with a Dual-Luciferase Reporter Assay System (Promega) using Lumat LB9507 (Berthold, Bad Wildbad, Germany). The pRL-CMV vector (Promega) was used to normalize the transfection efficiency of each assay.

2.10. *Chromatin immunoprecipitation (ChIP) assay*

The ovarian granulosa cells obtained from four or five mice were cultured in a 10-cm^2 dish for 4-5 days. After a wash with PBS, the cells were fixed by adding 1% formaldehyde in Opti-MEM (Invitrogen) for 10 min at room temperature with gentle agitation. For preparing the adult liver sample, 50 mg tissue was homogenized and crosslinked in Opti-MEM containing 1% formaldehyde. Glycine solution was added into the medium at a final concentration of 0.125M and incubated for 5 min to stop the crosslink reaction. After being washed twice with ice-cold PBS, the cells were harvested in 1 ml ice-cold PBS containing 1×proteinase inhibitor cocktail (Roche Molecular Biochemicals) and centrifuged at 700×g at 4°C for 5 min. The cells were lysed in SDS Lysis buffer (1% SDS, 10 mM EDTA, 50 mM Tris-HCl, pH 8.1) containing

1×proteinase inhibitor cocktail and incubated on ice for 10 min. The crosslinked chromatins from the granulosa cell and liver were sonicated using a Tomy Ultrasonic Disrupter UD-201 (Tomy, Tokyo, Japan) with 20% output for 15 sec 8 times. This generated DNA fragments of 200-1000 bp as was checked by agarose gel electrophoresis for each experiment. The chromatin was then centrifuged at 15,000 rpm at 4°C for 10 min and the supernatant was mixed with 9 volumes of ChIP Dilution buffer (0.01% SDS, 1.1 % Triton X-100, 1.2 mM EDTA, 16.7 mM Tris-HCl, 167 mM NaCl, pH 8.1) containing 1×proteinase inhibitor cocktail. In order to remove non-specific bindings, 120 μl protein G sepharose (GE healthcare) was added and incubated at 4°C for 1 h with rotation. After centrifugation at 2,000×g at 4°C for 1 min, the supernatant was collected in new tubes and 0.3 % of it was removed as an input fraction. The pre-cleared chromatin was separated into three portions and each incubated at 4°C for overnight with monoclonal antibodies specific for anti-dimethylated lysine 4 of histone H3 or anti-acetylated lysines 9 and 27 of histone H3 or 30 μg of normal mouse IgG. The antibodies for modified histones were kindly gifted by Dr. Hiroshi Kimura at Osaka University (Kimura et al., 2008). The immunocomplexes were incubated with 60 μl protein G sepharose for 1 h at 4°C with rotation followed by centrifugation at 4,000×g for 1 min at 4°C. The sepharose beads were then washed for 5 min each with Low Salt Wash buffer (150 mM NaCl, 0.1 % SDS, 1 % Triton X-100, 2 mM EDTA, 20 mM Tris-HCl, pH 8.1), High Salt Wash buffer (500 mM NaCl, 0.1 % SDS, 1 % Triton X-100, 2 mM EDTA, 20 mM Tris-HCl, pH 8.1), LiCl Wash buffer (0.25 M LiCl, 1 % NP40, 1 % sodium deoxycholate, 1 mM EDTA, 10 mM Tris-HCl, pH 8.1), and finally twice with TE buffer (10 mM Tris-HCl, 1 mM EDTA, pH 8.0). The chromatin was eluted twice with freshly prepared Elution buffer (1 % SDS, 0.1 M $NaHCO_3$) and subjected to reverse crosslinking with 0.2 M NaCl at 65°C for 4 h. The DNA was purified by phenol/CIAA extraction and ethanol precipitation and dissolved in TE buffer. The real-time PCR was performed as described above by using primer pairs listed in Table 1. The positions of the

primers for the two CGIs are shown in Fig. 1 (gray arrows). Histone modification levels were calculated as a ratio of the signal intensity of the immunoprecipitated fraction to that of the input fraction. Each ratio was normalized to the comparable signal detected at the ubiquitously expressed *Aip* promoter (defined as 1.0). The experiments were performed using three independent sets of the granulosa cell and adult liver.

2.11. *Statistical analysis*

Results were expressed as the average ± SD of multiple (n≥3) independent experiments. Student's *t* test was performed using Microsoft Excel statistical analysis functions (Microsoft Corp., Redmond, WA). Chi-square tests were used to compare the methylation rate of each CpG in the blastocyst, granulosa cell, and placenta with that in the liver and determine differentially methylated CpGs in the bisulfite sequencing analysis. Differences were considered statistically significant at $P < 0.05$.

3. Results

3.1. *Murine POP mRNA was highly expressed in the ovary, placenta, and blastocyst.*

We investigated the *POP* mRNA expression in mouse tissues related to reproduction and development (ovary, placenta, testis, and uterus) by qRT-PCR analysis (Fig. 2A). The liver was also assessed as a control of non-reproductive origin because it is a relatively homogeneous tissue and easily available in large amounts. We used three genes as internal controls to accurately estimate the *POP* mRNA level. *GAPDH* and *β-actin* are two of the most commonly used controls and *Aip* is a recently reported gene whose expression is stable under many conditions in many tissues (Frericks and Esser, 2008). The results showed different patterns of

POP mRNA expression depending on the normalizing control (Supplementary Fig. 1), presumably because the control genes are expressed at different levels in these tissues. To avoid bias, we calculated the average of the values obtained for the three controls (Fig. 2A). The ovary and placenta expressed a significantly higher level of *POP* mRNA than the liver while the testis and uterus did not. This strongly suggests that the ovary and placenta express the highest level of *POP* mRNA in the five tissues assessed. To determine the cell type expressing *POP* mRNA in the ovary and placenta we performed the *in situ* hybridization. Consistent with our previous study showing the porcine *POP* localization (Kimura et al., 1998), we detected the mouse *POP* mRNA exclusively in the granulosa cell (Fig. 2B). In the E17.5 placenta, a strong signal was observed only in the spongiotrophoblast layer (Fig. 2C). The identification of the spongiotrophoblast layer was performed by hybridization with its marker gene *Flt1* using the neighboring section (Hitz et al., 2005). No signal was observed in the sections hybridized with sense probes. Because the granulosa cell can be easily isolated, we assessed the *POP* mRNA level in the cell and found that it was about 18 times as high as the hepatic level when normalized to *GAPDH* (Fig. 2D). Using *β-actin* as a normalizing control, the *POP* mRNA level in the granulosa cell was about 9-fold higher than that in the liver (Supplementary Fig. 2A).

We next examined the *POP* mRNA expression at different developmental stages of mouse embryos and placentas by qRT-PCR analysis (Fig. 3A). In embryos, signal was first detected in unfertilized eggs indicating the presence of *POP* mRNA as a maternal RNA in the oocyte. The *POP* mRNA was not detected in 2-cell stage embryos but appeared in 3-4 cell stage embryos and its level reached a peak at the blastocyst stage. The blastocyst embryo showed the highest level of *POP* mRNA expression in the entire mouse development, 40 times as high as that in the liver when normalized to *GAPDH*. The *POP* mRNA expression then decreased at E6.5, rose again at E7.5 and E8.5, and decreased at E10.5. We used *β-actin* as another internal control and obtained similar results (Supplementary Fig. 2B). Northern blot analysis was conducted with

E9.5-E18.5 embryos and the *POP* signal was detected at all stages assessed (Fig. 3B). By normalizing the *POP* signal intensity with *GAPDH* mRNA signals, the embryonic *POP* mRNA was found to be expressed at an approximately constant level from E9.5 through E18.5 (Fig. 3B). The placental *POP* signal was also constant at E10.5-E18.5 (Fig. 3C).

3.2. *DNA methylation in the blastocyst, ovary, placenta, and liver.*

As shown in Figs. 2 and 3, *POP* mRNA is expressed at different levels in various tissues. This suggests that *POP* mRNA expression is controlled differently in each tissue. To assess one mechanism controlling the transcription, we investigated the DNA methylation status at the mouse *POP* locus. As we found two CGIs, namely CGI-1 and CGI-2, at the locus (Fig. 1), we examined the methylation in both these regions.

We applied bisulfite sequencing to genomic DNA samples from the blastocyst, ovarian granulosa cell, E18.5 placenta, and adult liver. Twenty subclones from each sample were sequenced and we checked which cytosine was converted to thymine. The percentage of non-CpG cytosines converted to a thymine was more than 99% in every data set indicating that the bisulfite reaction was successful (data not shown). In the CGI-1 region, almost all the CpG cytosines were found to be demethylated in all the tissues examined and their methylation rates were lower than 1% (Supplementary Fig. 3). We did not observe any difference in methylation of the CGI-1 region among these tissues. In contrast, the CGI-2 region contained many more methylated cytosines and methylation patterns differed between the four tissues (Fig. 4A). The overall percentage of methylated CpGs was 84.2% in the blastocyst, 86.4% in the granulosa cell, 80.3% in the placenta, and 96.5% in the liver. To determine which CpGs could be considered to be differentially methylated, we used chi-square analysis. We tested whether the methylation rate of each CpG in the blastocyst, granulosa cell, and placenta is significantly different from that in the liver. As a result, we identified, as differentially methylated CpGs, CpG#1, 2, 5, and

21 in the blastocyst, CpG#21, 32, and 33 in the granulosa cell, and CpG#1, 21, 26, 29, and 30 in the placenta (Figs. 4A and B). Interestingly, the percentage of methylated CpGs differed quite markedly according to sequenced subclones. In the blastocyst, no methylated cytosines were detected in two subclones whereas in most of the other subclones more than 90% of CpGs were methylated (Fig. 4A). In the granulosa cell and placenta, the methylation rate of each subclone varied from 39% to 97% and from 52% to 97% respectively. By contrast, in adult liver, more than 90% of CpGs were methylated in all the subclones.

3.3. *Effect of CGI-2 methylation on the POP promoter activity.*

We tested whether DNA methylation in the CGI-2 sequence affects the *POP* promoter activity by conducting an *in vitro* reporter analysis. We used a 914-bp *Eco*RI-*Bam*HI fragment (Fig. 1) as a potential promoter because it could activate a reporter gene *in vitro* (Kimura et al., 1999). The results showed that *POP* mRNA levels were 40- and 18-fold higher in the blastocyst and granulosa cell than liver respectively (Figs. 2D and 3A), while the DNA methylation level in the CGI-2 region differed by at most 60-65% between these tissues (Fig. 4, CpG#1 in the blastocyst and liver, CpG# 33 in the granulosa cell and liver, CpG#29 in the placenta and liver). It is worth examining whether the 60-65% difference in the DNA methylation rate of some CpGs in the CGI-2 region could cause the 40- or 18-fold difference in *POP* mRNA expression. Because it is technically difficult to generate a construct in which a specific CpG is methylated, we methylated the entire CGI-2 sequence *in vitro*. We prepared linear constructs as indicated in Figs. 5A and B and assessed their luciferase activities in the two mouse cell lines. The quantity and quality of the constructs were evaluated by agarose gel electrophoresis (Fig. 5C). The state of the constructs was checked with the methylation-sensitive *Hha*I restriction enzyme and by bisulfite sequencing (Figs. 5D and E). CGI-2 was found to enhance *POP* promoter activity (Fig. 5A) and its effect was significantly reduced by methylation in both cell lines (Fig. 5B). However,

we did not observe any difference in luciferase activity between the constructs containing CGI-2 methylated at 50% and 100%. As described by others (Tomikawa et al., 2006), the luciferase activity decreased on cutting out the CGI-2 fragment and religating it to the original vector although the mechanisms are not clear (compare the luciferase activity of mPOP-CG2-Linear in Fig. 5A with that of mPOP-CG2-0%me in Fig. 5B). These results indicate that the DNA methylation of the CGI-2 region could significantly reduce the *POP* promoter activity but the effect was not comparable to the difference in *POP* mRNA levels.

3.4. *Histone H3 acetylation and H3K4 methylation patterns in the ovary and liver.*

To further understand the role of CGIs in the *POP* regulation, we investigated histone modification patterns in the granulosa cell and liver. We assessed histone H3 acetylation and H3K4 methylation by ChIP assay because the two epigenetic marks are consistently associated with gene activation (Peterson and Laniel, 2004). We prepared five primer sets at the *POP* locus (Fig. 6A) and the modification levels were calculated as the ratio of DNA in the antibody-bound chromatin to that in the input fraction. To normalize the data from each ChIP, we used the promoter of the *Aip* gene which was expressed at similar levels in the granulosa cell and liver by our qRT-PCR analysis (data not shown). The *GAPDH* promoter showed only background levels of modifications, possibly because it is devoid of nucleosomes. The promoter (CGI-1) was highly acetylated and methylated in both the granulosa cell and liver and their modification levels were comparable to those of the *Aip* and *β-actin* promoters (Figs. 6B and C). We did not observe any significant differences in the modification levels between the two tissues. In contrast, CGI-2 was highly modified in the granulosa cell but not in the liver (Figs. 6B and C). The histone H3 acetylation and H3K4 methylation levels of CGI-2 in the granulosa cell were 6.1- and 3.7-fold higher than those in the liver respectively. Analysis of the data by Student's *t* test indicated that the histone H3 acetylation level in the granulosa cell is significantly higher

than that in the liver. The immunoprecipitation with normal mouse IgG resulted in background levels of modifications in all the regions (data not shown). These results suggest that CGI-2 plays a role in the high *POP* expression in the ovarian granulosa cell.

3.5. *Expression patterns of the neighboring genes.*

We finally considered the possibility that CGI-2 might be a regulator for the neighboring genes. Therefore, we investigated the expression of genes surrounding *POP*. The Ensembl database (http://www.ensembl.org/index.html) indicated the presence of six protein coding genes (*Atg5*, *Prdm1*, *Popdc3*, *Bves*, *Lin28b*, *Hace1*) other than *POP (Prep)* within a 2Mb region at mouse chromosome 10B2 (Fig. 7A). We first conducted 30 cycles of RT-PCR to see if these genes are expressed in the liver, ovary, and placenta. As a result, we detected no significant bands for the *Bves* and *Lin28b* genes and the signals for the *Prdm* and *Popdc3* genes were observed only in the placenta (Fig. 7B). Although the *Lin28b* gene was reported to be expressed almost exclusively in the placenta (Guo et al, 2006), we could not detect the signal. This might be because the expression level was below the detection limit in our analysis. In any event, the expression patterns of the four genes are not consistent with the epigenetic status of CGI-2. On the other hand, we detected the expression of the *Atg5* gene in all three tissues and the *Hace1* gene in the ovary and placenta (Fig. 7B). The expression pattern of the *Hace1* gene is in agreement with a previous report (Anglesio et al., 2004).

We then performed qRT-PCR analysis to determine expression levels of the *Atg5* and *Hace1* genes (Fig. 7C). As in Fig. 2A, the expression level of each gene was separately normalized to *GAPDH*, *β-actin*, and *Aip* genes and the average of the three values was calculated. Data normalized to each control is presented in Supplementary Fig. 4. The *Atg5* mRNA was expressed at a higher level in the liver and placenta than in the ovary and granulosa cell (Fig. 7C), suggesting that CGI-2 does not control the *Atg5* gene expression. In contrast, the *Hace1*

gene was expressed at significantly higher levels in the ovary, placenta, and the granulosa cell than in the liver (Fig. 7C). Although *Hace1* is unlikely to be a granulosa cell-specific gene because the mRNA level was higher in the whole ovary than in the granulosa cell, the pattern is consistent with the epigenetic status of CGI-2. This suggests that CGI-2 might regulate the expression of the *Hace1* gene which is located approximately 600 kb downstream. Taken together, the expression pattern of the five genes surrounding *POP* was not consistent with the epigenetic status of CGI-2, but we can not rule out the possibility that the CGI-2 region may be a regulator for the *Hace1* gene.

4. Discussion

4.1. *POP expression in the mouse embryonic development.*

In this study, we reported *POP* expression during the entire mouse embryonic development (Fig. 3). There are some studies reporting POP expression in late gestation and early postnatal development. In the rat brain, the POP activity and its mRNA expression remained high from E21 to 2 weeks after birth and gradually decreased thereafter (Agirregoitia et al., 2003; Fuse et al., 1990; Kato et al., 1980; Yamanaka et al., 1999). In the microsomal fraction of rat liver, the POP activity reached the peak at 2 weeks of age and then declined (Matsubara et al., 1998). The *POP* mRNA decreased during maturation of the mouse testis (Kimura et al., 2002). All of these data indicated that POP expression is high early in the development of the tissues. Our current data extended this observation and demonstrated that the embryonic *POP* expression dynamically changed throughout gestation. Interestingly, a similar fluctuation of the POP activity was recently reported during cerebellar granule cell differentiation in which the activity increased every 7 days (Moreno-Baylach et al. 2008). Although it could be due to intracellular

migration of the POP protein, the activity might also be regulated at the transcriptional level. Taken together, the results strongly suggest that *POP* expression is tightly controlled during embryonic development.

The *POP* mRNA was present at a high level in the unfertilized egg, blastocyst and, E7.5-E8.5 embryos (Fig. 3A), suggesting its importance at these stages. The unfertilized egg generally accumulates maternal RNA which is necessary for fertilization and early development. Because zygotic transcription begins at the two-cell stage in mice (O'Farrell et al., 2004) and until then the *POP* maternal mRNA was used up (Fig. 3A), POP is presumed to function in fertilization and/or the first cleavage of the fertilized egg. Indeed, a specific POP inhibitor suppressed fertilization and the first cleavage in the ascidian (Yokosawa et al., 1983, 1989). The blastocyst stage is when cells differentiate into trophectoderm and inner cell mass lineages (Rossant and Cross, 2001) and POP might have a role in the differentiation. The high *POP* expression at E7.5-E8.5 might be involved in drastic morphological changes around these stages. These suggest that POP plays some roles in cell division and tissue differentiation, as supported by studies with a POP-specific inhibitor. In the flesh fly and mouse, the inhibitor significantly prevented imaginal disc differentiation and fibroblast cell proliferation (Ishino et al., 1998; Ohtsuki et al., 1994). The administration of the inhibitor suppressed rat liver regeneration (Yamakawa et al., 1994). POP is likely to be involved in a series of differentiation events during embryogenesis.

4.2. *Regulation of the mouse POP gene expression.*

The mechanism controlling *POP* gene expression has been poorly understood. The only published experiment about *POP* gene regulation is an *in vitro* reporter analysis which identified a 200-bp region as a potential minimum promoter (Kimura et al., 1999). The current study investigated the DNA methylation and histone modification of CGIs to elucidate the epigenetic

control of *POP* gene expression. Our data clearly demonstrated that the mouse *POP* promoter (CGI-1) was completely hypomethylated in all the tissues examined (Supplementary Fig. 3). This is consistent with other reports that the state of the promoter is directly linked to gene expression. The promoters of *hprt, MAGE, Maspin, SF1,* and *protocadherin-α* are all methylated at silent loci but unmethylated when the genes are actively expressed (Chim et al., 2005; De Smet et al., 1999; Hoivik et al., 2008; Hornstra and Yang, 1994; Kawaguchi et al., 2008). The data also showed that the promoter was enriched in histone H3 acetylation and H3K4 methylation in both the granulosa cell and liver (Fig. 6), which is in agreement with previous studies. Active promoters of *Osteocalcin*, *Adiponectin*, *Collagenase*, and *Insulin* are associated with histone H3 acetylation and/or H3K4 methylation (Francis et al., 2005; Martens et al., 2003; Musri et al., 2006; Shen et al., 2002). These results clearly indicate that the epigenetic state at the promoter is essential for gene activation. In the case of the *POP* gene, DNA demethylation and histone acetylation and H3K4 methylation of the promoter probably play a central role in its activation. The mechanisms by which a gene with a hypomethylated promoter is activated are not fully understood. A transcription factor Sp1 may be involved in the gene activation by a mechanism similar to that observed for the *Aprt* gene because the *POP* promoter contains several Sp1-binding sites (Brandeis et al., 1994; Macleod et al., 1994).

We found that DNA methylation of the CGI-2 region differed among the blastocyst, ovarian granulosa cell, placenta, and liver (Fig. 4). Many sequences distal from promoters have been shown to be methylated at different levels in different tissues and be implicated in gene regulation. One of the most studied loci is the imprinting control region (ICR) of *Igf2* and *H19* in which the differentially methylated ICR regulates allele-specific gene expression (Edwards and Ferguson-Smith, 2007). Several genes expressed in male germ cells have been suggested to be controlled by tissue-dependent and differentially methylated regions other than promoters (Suzuki et al., 2007). These results supported the idea that the differentially methylated CGI-2

region is involved in the regulation of *POP* mRNA expression. Considering that *POP* is expressed in most tissues at various levels, CGI-2 might control its mRNA level rather than activation and silencing of the gene. We tested this hypothesis and assessed whether the DNA methylation of CGI-2 could cause the 40- or 18-fold difference in the *POP* mRNA level between the blastocyst, granulosa cell, and liver. However, the reporter analysis indicated that the *POP* promoter activity was reduced by 30-40% only when the CGI-2 methylation rate was increased from 0% to 50% or 0% to 100%, and methylation rates of 50% and 100% did not make any difference (Fig. 5B). Because only a few subclones from blastocysts were completely hypomethylated in the bisulfite sequencing analysis, *POP* mRNA expression might be affected by CGI-2 methylation in only a few cells of the blastocyst (Fig. 4). Obviously this could not cause the 40-fold difference in *POP* mRNA expression, suggesting CGI-2 methylation to have only a minor effect on the gene regulation. The reason why CGI-2 was completely hypomethylated in some cells of the blastocyst is not known. It might reflect the different cell types included in the blastocyst or be due to variation within a single cell type. Alternatively, it might be sex differences as reported in the promoter of estrogen and progesterone receptor genes (McCarthy et al., 2009).

It is also possible that methylation of specific CpGs in CGI-2 may have an effect on *POP* expression. There are some examples in which methylation rates of a few CpGs in a CGI are correlated with gene expression (Li et al., 2008; Tomikawa et al., 2004). A very recent report provided evidence that methylation of a single CpG dinucleotide in a CGI is functionally linked to the *PMP24* gene expression (Zhang et al., 2010). These suggest that the differentially methylated CpGs in CGI-2 are possibly involved in the regulation of the *POP* gene. In our reporter analysis, CGI-2 methylation at 50% and 100% resulted in similar luciferase activities (Fig. 5B), potentially because methylation rates of the differentially methylated CpGs ,except for CpG#1 and 5, were similar between the constructs (Fig. 5E). In this scenario, transcription

factors binding to the CpGs would play an important role in the gene regulation. By a database search, USF, c-Myc, and GATA proteins were identified as potential transcription factors binding to the differentially methylated CpGs. Their binding affinity might be changed by methylation.

Even if specific CpGs are essential for *POP* expression, the dynamic change during embryonic development (Fig. 3A) is unlikely to be controlled by DNA methylation only. Generally, DNA methylation pattern is erased until 4-cell stage and re-established in the blastocyst embryo and the status is stable after that (Shi and Wu, 2009). Therefore, the fluctuation of *POP* expression after implantation is presumably regulated by other factors. This implies that histone modifications are involved in the regulation of the *POP* gene. We then investigated histone H3 acetylation and H3K4 methylation and found that CGI-2 was highly modified in the ovarian granulosa cell but not in the liver (Fig. 6). The two epigenetic marks have been shown to be linked to the activities of many *cis*-elements. A 3' enhancer for *Snail* gene was associated with histone H3 acetylation and H3K4 methylation and thereby could activate its transcription in melanoma cells (Palmer et al., 2007). A transcription factor FoxA1 requires histone H3K4 methylation for binding to distal enhancers (Lupien et al., 2008). Formation of the histone hyperacetylated domain at the locus control region is crucial for activation of the β-globin and human growth hormone gene cluster (Bulger, 2005; Kimura et al., 2007). These studies show that a regulatory region critical for gene activation is consistently associated with histone acetylation and H3K4 methylation in the tissue or cell expressing the gene. Our ChIP analysis revealed an enrichment of histone H3 acetylation and H3K4 methylation in the CGI-2 region exclusively in the granulosa cell (Fig. 6). Considering that CGI-2 has an enhancer activity in the *in vitro* reporter gene assay (Fig. 5A), the results suggest that CGI-2 is a novel regulator responsible for the high *POP* expression in the granulosa cell.

Our results suggested some correlation between the epigenetic status of CGI-2 and the *POP*

mRNA level. However, it is not clear from our data how important the CGI-2 sequence is for *POP* expression. The difference of epigenetic status in the CGI-2 region was small compared with that of *POP* mRNA levels in various tissues and CGI-2 may even be a regulator for the *Hace1* gene. The presence of other regulatory sequences is possible and further study will be required to clarify this issue.

5. Conclusions

Murine *POP* mRNA was highly expressed in the ovarian granulosa cell, placental spongiotrophoblast, and blastocyst embryo. Epigenetic patterns at the promoter were similar among the tissues expressing *POP* at different levels, suggesting the DNA methylation and histone modification at the promoter are important for the *POP* gene activation. Some CpGs in CGI-2 was demethylated in the tissues expressing a high level of *POP* mRNA and the histone H3 acetylation and H3K4 methylation levels in CGI-2 were higher in the granulosa cell than in the liver. Because the CGI-2 sequence increased the *POP* promoter activity *in vitro* and its effect was reduced by DNA methylation, it might work as an enhancer for *POP* expression. Although it is possible that CGI-2 may regulate another gene, our data suggest that CGI-2 plays a role in the regulation of *POP* expression. Further study will be required to elucidate the *in vivo* activity of CGI-2 and to find other regulatory elements.

Acknowledgements

We thank Dr. Hiroshi Kimura (Osaka University) for kindly gifting the antibodies against

modified histones. We also thank Dr. Katsushi Kagaya for advising on statistical analyses. We are grateful to Drs. Stephen A. Liebhaber, Nancy E. Cooke, Asato Kuroiwa, Katsueki Ogiwara, and Sanath Rajapakse for critical reading of the manuscript. This work was supported by Grants-in-aid for Scientific Research 19770048, 21770068 (A.P.K.) and 21370024, 21657019 (T.T.) from the Ministry of Education, Culture, Sports, Science and Technology, Japan.

References

Agirregoitia, N., Irazusta, A., Ruiz, F., Irazusta, J., Gil, J., 2003. Ontogeny of soluble and particulate prolyl endopeptidase activity in several areas of the rat brain and in the pituitary gland. Dev. Neurosci. 25, 316-323.

Anglesio, M.S., Evdokimova, V., Melnyk. N., Zhang, L., Fernandez, C.V., Grundy, P.E., Leach, S., Marra, M.A., Brooks-Wilson, A.R., Penninger, J., Sorensen, P.H. 2004. Differential expression of a novel ankyrin containing E3 ubiquitin-protein ligase, Hace1, in sporadic Wilms' tumor versus normal kidney. Hum. Mol. Genet. 13, 2061-2074.

Bellemère, G., Vaudry, H., Mounien, L., Boutelet, I., Jégou, S., 2004. Localization of the mRNA encoding prolyl endopeptidase in the rat brain and pituitary. J. Comp. Neurol. 471, 128-143.

Berger, S.L., 2002. Histone modifications in transcriptional regulation. Curr. Opin. Genet. Dev. 12,142-148.

Brandeis, M., Frank, D., Keshet, I., Siegfried, Z., Mendelsohn, M., Nemes, A., Temper, V., Razin, A., Cedar, H., 1994. Sp1 elements protect a CpG island from de novo methylation. Nature 371, 435-438.

Bulger, M., 2005. Hyperacetylated chromatin domains: lessons from heterochromatin. J. Biol. Chem. 280, 21689-21692.

Caiafa, P., Zampieri, M., 2005. DNA methylation and chromatin structure: the puzzling CpG islands. J. Cell Biochem. 94, 257-265.

Cedar, H., Bergman, Y., 2009. Linking DNA methylation and histone modification: patterns and paradigms. Nat. Rev. Genet. 10, 295-304.

Chim, S.S., Tong, Y.K., Chiu, R.W., Lau, T.K., Leung, T.N., Chan, L.Y., Oudejans, C.B., Ding, C., Lo, Y.M., 2005. Detection of the placental epigenetic signature of the maspin gene in maternal plasma. Proc. Natl. Acad. Sci. U.S.A. 102, 14753-14758.

Choi, J.K., Howe, L.J., 2009. Histone acetylation: truth of consequences? Biochem. Cell Biol. 87, 139-150.

De Smet, C., Lurquin, C., Lethé, B., Martelange, V., Boon, T., 1999. DNA methylation is the primary silencing mechanism for a set of germ line- and tumor-specific genes with a CpG-rich promoter. Mol. Cell. Biol. 19, 7327-7335.

Di Daniel, E., Glover, C.P., Grot, E., Chan, M.K., Sanderson, T.H., White, J.H., Ellis, C.L., Gallagher, K.T., Uney, J., Thomas, J., Maycox, P.R., Mudge, A.W., 2009. Prolyl oligopeptidase binds to GAP-43 and functions without its peptidase activity. Mol. Cell. Neurosci. 41, 373-382.

Edwards, C.A., Ferguson-Smith, A.C., 2007. Mechanisms regulating imprinted genes in clusters. Curr. Opin. Cell Biol. 19, 281-289.

Fraczek, J., Kim, T.W., Xiao, H., Yao, J., Wen, Q., Li, Y., Casanova, J.L., Pryjma, J., Li, X., 2008. The kinase activity of IL-1 receptor-associated kinase 4 is required for interleukin-1 receptor/toll-like receptor-induced TAK1-dependent NFkappaB activation. J. Biol. Chem. 283, 31697-31705.

Francis, J., Chakrabarti, S.K., Garmey, J.C., Mirmira, R.G., 2005. Pdx-1 links histone H3-Lys-4 methylation to RNA polymerase II elongation during activation of insulin transcription. J. Biol. Chem. 280, 36244-36253.

Frericks, M., Esser, C., 2008. A toolbox of novel murine house-keeping genes identified by meta-analysis of large scale gene expression profiles. Biochim. Biophys. Acta 1779, 830-837.

Fuse, Y., Polk, D.H., Lam, R.W., Reviczky, A.L., Fisher, D.A., 1990. Distribution and ontogeny of thyrotropin-releasing hormone degrading enzymes in rats. Am. J. Physiol. 259, E787-E791.

Garcia-Horsman, J.A., Männistö, P.T., Venäläinen, J.I., 2007. On the role of prolyl oligopeptidase in health and disease. Neuropeptides 41, 1-24.

Goossens, F., De Meester, I., Vanhoof, G., Scharpé, S., 1996. Distribution of prolyl oligopeptidase in human peripheral tissues and body fluids. Eur. J. Clin. Chem. Clin. Biochem. 34, 17-22.

Guo, Y., Chen, Y., Ito, H., Watanabe, A., Ge, X., Kodama, T., Aburatani, H., 2006. Identification and characterization of lin-28 homolog B (LIN28B) in human hepatocellular carcinoma. Gene 384, 51-61.

Hitz, C., Vogt-Weisenhorn, D., Ruiz, P., Wurst, W., Floss, T., 2005. Progressive loss of the spongiotrophoblast layer of Birc6/Bruce mutants results in embryonic lethality. Genesis 42, 91-103.

Hoivik, E.A., Aumo, L., Aesoy, R., Lillefosse, H., Lewis, A.E., Perrett, R.M., Stallings, N.R., Hanley, N.A., Bakke, M., 2008. Deoxyribonucleic acid methylation controls cell type-specific expression of steroidogenic factor 1. Endocrinology 149, 5599-5609.

Hornstra, I.K., Yang, T.P., 1994. High-resolution methylation analysis of the human hypoxanthine phosphoribosyltransferase gene 5' region on the active and inactive X chromosomes: correlation with binding sites for transcription factors. Mol. Cell. Biol. 14, 1419-1430.

Hublitz, P., Albert, M., Peters, A.H., 2009. Mechanisms of transcriptional repression by histone

lysine methylation. Int. J. Dev. Biol. 53, 335-354.

Illingworth, R.S., Bird, A.P., 2009. CpG islands--'a rough guide'. FEBS Lett. 583, 1713-1720.

Irazusta, J., Larrinaga, G., González-Maeso, J., Gil, J., Meana, J.J., Casis, L., 2002. Distribution of prolyl endopeptidase activities in rat and human brain. Neurochem. Int. 40, 337-345.

Ishino, T., Ohtsuki, S., Homma, K., Natori, S., 1998. cDNA cloning of mouse prolyl endopeptidase and its involvement in DNA synthesis by Swiss 3T3 cells. J. Biochem. 123, 540-545.

Kato, T., Nakano, T., Kojima, K., Nagatsu, T., Sakakibara, S., 1980. Changes in prolyl endopeptidase during maturation of rat brain and hydrolysis of substance P by the purified enzyme. J. Neurochem. 35, 527-535.

Kawaguchi, M., Toyama, T., Kaneko, R., Hirayama, T., Kawamura, Y., Yagi, T., 2008. Relationship between DNA methylation states and transcription of individual isoforms encoded by the protocadherin-alpha gene cluster. J. Biol. Chem. 283, 12064-12075.

Kimura, A., Ohnishi, J., Okimura, H., Hamabata, T., Takahashi, T., 1998. Localization of prolyl endopeptidase mRNA in small growing follicles of porcine ovary. Mol. Reprod. Dev. 50, 121-127.

Kimura, A., Yoshida, I., Takagi, N., Takahashi, T., 1999. Structure and localization of the mouse prolyl oligopeptidase gene. J. Biol. Chem. 274, 24047-24053.

Kimura, A., Matsui, H., Takahashi, T., 2002. Expression and localization of prolyl oligopeptidase in mouse testis and its possible involvement in sperm motility. Zool. Sci. 19, 93-102.

Kimura, A.P., Sizova, D., Handwerger, S., Cooke, N.E., Liebhaber, S.A., 2007. Epigenetic activation of the human growth hormone gene cluster during placental cytotrophoblast differentiation. Mol. Cell. Biol. 27, 6555-6568.

Kimura, H., Hayashi-Takanaka, Y., Goto, Y., Takizawa, N., Nozaki, N., 2008. The organization

of histone H3 modifications as revealed by a panel of specific monoclonal antibodies. Cell Struct. Funct. 33, 61-73.

Kwon, I., Lee, J., Chang, S.H., Jung, N.C., Lee, B.J., Son, G.H., Kim, K., Lee, K.H., 2006. BMAL1 shuttling controls transactivation and degradation of the CLOCK/BMAL1 heterodimer. Mol. Cell. Biol. 26, 7318-7330.

Li, D., Da, L., Tang, H., Li, T., Zhao, M., 2008. CpG methylation plays a vital role in determining tissue- and cell-specific expression of the human cell-death-inducing DFF45-like effector A gene through the regulation of Sp1/Sp3 binding. Nucleic Acids Res. 36, 330-341.

Lupien, M., Eeckhoute, J., Meyer, C.A., Wang, Q., Zhang, Y., Li, W., Carroll, J.S., Liu, X.S., Brown, M., 2007. FoxA1 translates epigenetic signatures into enhancer-driven lineage-specific transcription. Cell 132, 958-970.

Macleod, D., Charlton, J., Mullins, J., Bird, A.P., 1994. Sp1 sites in the mouse aprt gene promoter are required to prevent methylation of the CpG island. Genes Dev. 8, 2282-2292.

Martens, J.H., Verlaan, M., Kalkhoven, E., Zantema, A., 2003. Cascade of distinct histone modifications during collagenase gene activation. Mol. Cell. Biol. 23, 1808-1816.

Martin, C., Zhang, Y., 2005. The diverse functions of histone lysine methylation. Nat. Rev. Mol. Cell. Biol. 6, 838-849.

Matsubara, Y., Ono, T., Tsubuki, S., Irie, S., Kawashima, S., 1998. Transient up-regulation of a prolyl endopeptidase activity in the microsomal fraction of rat liver during postnatal development. Eur. J. Biochem. 252, 178-183.

McCarthy, M.M., Auger, A.P., Bale, T.L., De Vries, G.J., Dunn, G.A., Forger, N.G., Murray, E.K., Nugent, B.M., Schwarz, J.M., Wilson, M.E., 2009. The epigenetics of sex differences in the brain. J. Neurosci. 29, 12815-12823.

Moreno-Baylach, M.J., Felipo, V., Männistö, P.T., García-Horsman, J.A., 2008. Expression and

traffic of cellular prolyl oligopeptidase are regulated during cerebellar granule cell differentiation, maturation, and aging. Neuroscience 156, 580-585.

Musri, M.M., Corominola, H., Casamitjana, R., Gomis, R., Párrizas, M., 2006. Histone H3 lysine 4 dimethylation signals the transcriptional competence of the adiponectin promoter in preadipocytes. J. Biol. Chem. 281, 17180-17188.

Myöhänen, T.T., Venäläinen, J.I., Tupala, E., Garcia-Horsman, J.A., Miettinen, R., Männistö, P.T., 2007. Distribution of immunoreactive prolyl oligopeptidase in human and rat brain. Neurochem. Res. 32, 1365-1374.

Myöhänen, T.T., Venäläinen, J.I., Garcia-Horsman, J.A., Männistö, P.T., 2008a. Spatial association of prolyl oligopeptidase, inositol 1,4,5-triphosphate type 1 receptor, substance P and its neurokinin-1 receptor in the rat brain: an immunohistochemical colocalization study. Neuroscience 153, 1177-1189.

Myöhänen, T.T., Venäläinen, J.I., Garcia-Horsman, J.A., Piltonen, M., Männistö, P.T., 2008b. Cellular and subcellular distribution of rat brain prolyl oligopeptidase and its association with specific neuronal neurotransmitters. J. Comp. Neurol. 507, 1694-1708.

Myöhänen, T.T., García-Horsman, J.A., Tenorio-Laranga, J., Männistö, P.T., 2009. Issues about the physiological functions of prolyl oligopeptidase based on its discordant spatial association with substrates and inconsistencies among mRNA, protein levels, and enzymatic activity. J. Histochem. Cytochem. 57, 831-848.

Nagy, A., Gertsenstein, M., Vintersten, K., Behringer, R., 2002. Manipulating the Mouse Embryo: A Laboratory Manual, third ed. Cold Spring Harbor, New York.

Ng, H.H., Bird, A., 1999. DNA methylation and chromatin modification. Curr. Opin. Genet. Dev. 9, 158-163.

O'Farrell, P.H., Stumpff, J., Su, T.T., 2004. Embryonic cleavage cycles: how is a mouse like a fly? Curr. Biol. 14, R35-R45.

Ohtsuki, S., Homma, K., Kurata, S., Komano, H., Natori, S., 1994. A prolyl endopeptidase of Sarcophaga peregrina (flesh fly): its purification and suggestion for its participation in the differentiation of the imaginal discs. J. Biochem. 115, 449-453.

Palmer, M.B., Majumder, P., Green, M.R., Wade, P.A., Boss, J.M., 2007. A 3' enhancer controls snail expression in melanoma cells. Cancer Res. 67, 6113-6120.

Perroud, B., Alvarado, R.J., Espinal, G.M., Morado, A.R., Phinney, B.S., Warden, C.H., 2009. In vivo multiplex quantitative analysis of 3 forms of alpha melanocyte stimulating hormone in pituitary of prolyl endopeptidase deficient mice. Mol. Brain 2, 14.

Peterson, C.L., Laniel, M.A., 2004. Histones and histone modifications. Curr. Biol. 14, R546-R551.

Rossant, J., Cross, J.C., 2001. Placental development: lessons from mouse mutants. Nat. Rev. Genet. 2, 538-548.

Schulz, I., Zeitschel, U., Rudolph, T., Ruiz-Carrillo, D., Rahfeld, J.U., Gerhartz, B., Bigl, V., Demuth, H.U., Rossner, S., 2005. Subcellular localization suggests novel functions for prolyl endopeptidase in protein secretion. J. Neurochem. 94, 970-979.

Shen, J., Montecino, M., Lian, J.B., Stein, G.S., Van Wijnen, A.J., Stein, J.L., 2002. Histone acetylation in vivo at the osteocalcin locus is functionally linked to vitamin D-dependent, bone tissue-specific transcription. J. Biol. Chem. 277, 20284-20292.

Shi, L., Wu, J., 2009. Epigenetic regulation in mammalian preimplantation embryo development. Reprod. Biol. Endocrinol. 7, 59.

Suzuki, M., Sato, S., Arai, Y., Shinohara, T., Tanaka, S., Greally, J.M., Hattori, N., Shiota, K., 2007. A new class of tissue-specifically methylated regions involving entire CpG islands in the mouse. Genes Cells 12, 1305-1314.

Takano, N., Matsui, H., Takahashi, T., 2004. TESSP-1: a novel serine protease gene expressed in the spermatogonia and spermatocytes of adult mouse testes. Mol. Reprod. Dev. 70, 1-10.

Tomikawa, J., Fukatsu, K., Tanaka, S., Shiota, K., 2006. DNA methylation-dependent epigenetic regulation of dimethylarginine dimethylaminohydrolase 2 gene in trophoblast cell lineage. J. Biol. Chem. 281, 12163-12169.

Walter, R., Shlank, H., Glass, J.D., Schwartz, I.L., Kerenyi, T.D., 1971. Leucylglycinamide released from oxytocin by human uterine enzyme. Science 173, 827-829.

Warden, C.H., Fisler, J.S., Espinal, G., Graham, J., Havel, P.J., Perroud, B., 2009. Maternal influence of prolyl endopeptidase on fat mass of adult progeny. Int. J. Obes. 33, 1013-1022.

Wilk, S., 1983. Prolyl endopeptidase. Life Sci. 33, 2149-2157.

Williams, R.S.B., 2004. Prolyl oligopeptidase and bipolar disorder. Clin. Neurosci. Res. 4, 233-242.

Yamakawa, N., Shimeno, H., Soeda, S., Nagamatsu, A., 1994. Regulation of prolyl oligopeptidase activity in regenerating rat liver. Biochim. Biophys. Acta 1199, 279-284.

Yamanaka, C., Lebrethon, M.C., Vandersmissen, E., Gerard, A., Purnelle, G., Lemaitre, M., Wilk, S., Bourguignon, J.P., 1999. Early prepubertal ontogeny of pulsatile gonadotropin-releasing hormone (GnRH) secretion: I. Inhibitory autofeedback control through prolyl endopeptidase degradation of GnRH. Endocrinology 140, 4609-4615.

Yokosawa, H., Miyata, M., Sawada, H., Ishii, S., 1983. Isolation and characterization of a post-proline cleaving enzyme and its inhibitor sperm of the ascidian, Halocynthia roretzi. J. Biochem. 94, 1067-1076.

Yokosawa, H., Nishikata, M., Ishii, S., 1989. Involvement of prolyl endopeptidase in ascidian fertilization. Experientia 45, 381-383.

Zhang, X., Wu, M., Xiao, H., Lee, M.T., Levin, L., Leung, Y.K., Ho, S.M., 2010. Methylation of a single intronic CpG mediates expression silencing of the PMP24 gene in prostate cancer. Prostate 70, 765-776.

Figure Legends

Fig. 1. Structure of the mouse *POP* gene and positions of probes and primers used in this study. Genomic organization of the mouse *POP (Prep)* gene is illustrated with its neighboring genes. Exons are represented by vertical lines and rectangles with the exon number. White boxes in exons 1 and 15 indicate 5' and 3' untranslated regions respectively while the black regions are protein coding sequences. The *Prdm1* and *Popdc3* genes are present 608 kb upstream and 130 kb downstream to the *POP* gene. Two CGIs (CGI-1 and CGI-2) are indicated with bold lines. Enlarged figures around exons 1 and 15 including each CGI are drawn at the top. Three transcriptional initiation sites were previously identified as shown by bent arrows. Positions of a 914-bp *Eco*RI-*Bam*HI fragment and a 690-bp CGI-2 region used for the reporter gene assay are indicated by gray bars. Arrows are the positions of the primers used for bisulfite sequencing (black) and ChIP analyses (gray). At the bottom, cDNA structure of *POP* is shown. A protein-coding region is represented by open boxes, and noncoding regions are represented by horizontal lines. Positions of the probes for *in situ* hybridization and Northern blot analyses are indicated with gray and black bars respectively. Arrows indicates the position of the primers for qRT-PCR analysis.

Fig. 2. The mouse *POP* mRNA was highly expressed in the ovarian granulosa cell and placental spongiotrophoblast layer. (A) qRT-PCR analysis of *POP* in the liver, ovary, placenta, testis, and uterus. Total RNA was prepared from the five tissues and one microgram of the RNA was used for reverse transcription. *POP* mRNA expression was analyzed by real time PCR using the ABI Prism 7300 real-time PCR system. *POP* mRNA levels were separately normalized to *GAPDH, β-actin,* and *Aip* and the average of them is shown as a graph. Relative expression is shown as

-fold difference calculated relative to the expression in the liver, which was arbitrarily set at 1.0. The data are presented as mean ± SD from four independent experiments with two tissues. n = 4; **, $P < 0.01$ compared with liver. (B) *In situ* hybridization analysis of *POP* in the mouse ovary. Frozen sections (10 μm) were prepared from the superovulated ovary. Neighboring sections were hybridized with DIG-labeled sense (SS) and antisense (AS) cRNA probes for *POP*. The signal was detected by using NBT/BCIP substrates. Follicles indicated in a box in the upper panel are shown below at higher magnification. *POP* was specifically expressed in the ovarian granulosa cell. The bar represents 300 μm (upper panels) or 100 μm (lower panels). (C) *In situ* hybridization analysis of *POP* in the mouse placenta. Frozen sections (10 μm) were prepared from the E17.5 placenta and the *POP* signal was detected as in (B). To identify the placental structure the probe for a spongiotrophoblast marker gene *Flt1* was also used. *POP* was strongly expressed in the placental spongiotrophoblast layer. Md, maternal decidua, Sp, spongiotrophoblast, La, labyrinth. The bar represents 1 mm. (D) Comparison of *POP* mRNA in the ovarian granulosa cell and liver. Total RNA was prepared from granulosa cells which were obtained with 3 superovulated mice. Three micrograms of the RNA was used for qRT-PCR analysis as in (A). *POP* mRNA levels were normalized to *GAPDH* and are represented as in (A). The data are presented as mean ± SD from four independent experiments with two sets of granulosa cells and two adult livers. n = 4; **, $P < 0.01$ compared with liver.

Fig. 3. *POP* mRNA expression patterns in the mouse embryo and placenta. (A) qRT-PCR analysis of *POP* in the embryos before E10.5. The embryos at E6.5-E10.5 were collected from pregnant mice and those before implantation were obtained by *in vitro* fertilization. Unfertilized eggs were collected by treating superovulated cumulus-oocyte complexes with hyaluronidase. The E18.5 placenta and adult liver were also assessed for comparison. Total RNA was isolated from each sample and *POP* mRNA expression was analyzed by qRT-PCR as in Fig. 2A. *POP*

mRNA levels were normalized to *GAPDH* and relative expression is shown as -fold difference calculated relative to the expression in the liver, which was arbitrarily set at 1.0. The data are presented as mean ± SD from at least three independent experiments with 44 unfertilized eggs, 2-24 embryos, or a placenta. $n = 3$ or 6; *, $P < 0.05$ and **, $P < 0.01$ compared with liver. (B, C) Northern blot analysis of *POP* in mouse embryos (B) and placentas (C). Total RNA was prepared from the embryo at stages E9.5 through E18.5 and the placenta at E10.5-E18.5. Twenty micrograms of the RNA was electrophoresed and blotted to a nylon membrane. The blot was hybridized with a ^{32}P-labeled mouse *POP* cDNA probe and the signals were detected by autoradiography. A probe for mouse *GAPDH* was used as an internal control. The intensity of each band was measured using the ImageJ program and *POP* mRNA levels relative to *GAPDH* levels are represented as a graph at the top. Relative expression is shown as -fold difference calculated relative to the expression in the E10.5 embryo (B) and E10.5 placenta (C), which was arbitrarily set at 1.0.

Fig. 4. DNA methylation patterns of the CGI-2 region in the blastocyst, granulosa cell, placenta, and liver. (A) Structure of the mouse *POP* gene and positions of CGI-1 and CGI-2 regions are drawn at the top. The mouse *POP* gene is about 92 kb long containing 15 exons and the first two and last two exons are depicted by open boxes with the exon number. A detailed map of the CGI-2 region and DNA methylation patterns in each tissue are shown below the gene structure. CGI-2 includes 33 CpG dinucleotides all of which were analyzed. The positions of the 33 CpG dinucleotides are shown with vertical lines. The state of individual CGIs was determined by bisulfite sequencing. Genomic DNA was purified from 14 blastocyst embryos, two 35-mm^2 dishes of granulosa cells, two E18.5 placentas, and two adult livers. The DNA was treated with sodium bisulfite and the CGI-2 region was amplified by PCR. For blastocyst samples, the second round of PCR was conducted with nested primers. Ten subclones of the amplified

product for each granulosa cell, E18.5 placenta, and adult liver, and twenty for the blastocyst were analyzed by DNA sequencing. Open and filled circles represent unmethylated and methylated cytocines, respectively. The overall methylation rate for each tissue is indicated at the left. Differentially methylated CpGs that were determined by chi-square analysis are marked with asterisks ($P < 0.05$). (B) The methylation rate of differentially methylated CpGs is shown as a graph. Each bar represents the percentage of a methylated CpG in the blastocyst (white), granulosa cell (light gray), E18.5 placenta (dark gray), and liver (black). *, $P < 0.05$ compared with liver.

Fig. 5. CpG methylation in the CGI-2 region significantly reduced the transcriptional activity of the *POP* promoter. (A, B) Reporter constructs and luciferase activities. The left panel shows a schematic drawing of the reporter gene constructs generated in this study. CGI-2 is indicated as 'CG2'. Gaps between the luciferase gene and CGI-2 region in (B) indicate that the CGI-2 fragment was cut out, methylated *in vitro* (0, 50, or 100%), and religated to the construct. The constructs were transfected into Hepa1-6 or NIH3T3-3-4 cells by lipofection. The measured luciferase activity is shown in graphs. The data are presented as mean ± SD from three independent experiments. $n = 3$; *, $P < 0.05$ compared with the mPOP-CG2-0%me construct in Hepa1-6 cells. $n = 3$; **, $P < 0.01$ compared with mPOP-CG2-0%me construct in NIH3T3-3-4 cells. (C) The amount of DNA and purity of each construct were evaluated by agarose gel electrophoresis and ethidium bromide staining. The picture shows that each linear construct was used at a similar amount for the assay. (D) *Hha*I-digestion patterns of methylated CGI-2. The 690bp CGI-2 fragment which included 0%, 50%, or 100% methylated CpG dinucleotides was digested with the methylation-sensitive *Hha*I restriction enzyme. The CGI-2 fragment contains two *Hha*I sites as shown in the schematic drawing at the bottom. Short vertical lines indicate the positions of CpGs. (E) Bisulfite sequencing of the two *in vitro* methylated constructs. 100-300

ng of each construct was used for bisulfite sequencing, and 4 subclones were sequenced. The positions of CpGs in the CGI-2 sequence are illustrated at the top. Open and filled circles represent unmethylated and methylated cytocines respectively. The differentially methylated CpGs are marked with asterisks. The methylation rates were 58.3% for mPOP-CG2-50%me and 95.5% for mPOP-CG2-100%me.

Fig. 6. Histone modification patterns at the mouse *POP* gene locus in the granulosa cell and adult liver. (A) A genomic structure of the mouse *POP* gene locus is illustrated. Exons are indicated by vertical lines or open boxes with the exon number. Two CGIs are represented by filled boxes. Positions of five primer pairs for ChIP were indicated by arrows. (B) Histone H3 acetylation pattern at the mouse *POP* locus. ChIP was conducted with chromatin isolated from the granulosa cell and liver. The sheared chromatin was immunoprecipitaed with a monoclonal antibody against acetylated histone H3K9K27 (H3K9K27ac). DNA purified from the precipitated (bound) fraction was subjected to real time PCR amplification using the primers shown in A. The amplification efficiency was normalized by calculating the ratio of the signal in the bound chromatin to that in the input fraction. The value was further normalized by the bound to input ratio of the constitutively active *Aip* gene promoter designated as 1.0. ChIP was performed three times with three sets of the granulosa cell and liver and we conducted duplicate PCR for each sample. The graph was shown as the average ± SD. The black bar represents the acetylation levels in the granulosa cell and the white bar in the liver. Student's *t* test indicates that the acetylation level of CGI-2 in the granulosa cell is significantly higher than that in the liver ($n = 6$; *, $P < 0.05$). (C) Histone H3K4 dimethylation pattern at the mouse *POP* locus. ChIP was conducted as in (B) using a monoclonal antibody against dimethylated histone H3K4 (H3K4me2). The methylation level was calculated and normalized as in (B).

Fig. 7. Expression patterns of six genes surrounding the *POP* gene. (A) A 2Mb region at mouse chromosome 10B2 including *POP (Prep)* is illustrated. There are seven protein coding genes in the region, each of which is depicted as a rectangle with the gene symbol. The direction of transcription of each gene is indicated by the arrow. (B) RT-PCR of the genes located on mouse chromosome 10B2 in the liver, ovary, and E18.5 placenta. Isolation of total RNA and reverse transcription were performed with (+) or without reverse transcriptase (-) as in Fig. 2A. 30 cycles of PCR was conducted and the signal was visualized by ethidium bromide staining after agarose gel electrophoresis. The results from two independently prepared cDNA for each tissue are shown. (C) qRT-PCR analysis of the *Atg5* and *Hace1* genes in the liver, ovary, placenta, and granulosa cell. Real-time PCR was conducted and the mRNA levels were calculated as in Fig. 2A. Relative expression is shown as -fold difference calculated relative to the expression in the liver, which was arbitrarily set at 1.0. The data are presented as mean ± SD from four independent experiments with two tissues. $n = 4$; *, $P < 0.05$ compared with liver. **, $P < 0.01$ compared with liver.

Table 1

Oligonucleotide primers used in this study.

Designation	Forward	Reverse
qRT-PCR		
mPOP	5’-GGAATCGATGCTGCTGATTA-3’	5’-CCATCCAGCTTTATGCCTTT-3’
mGAPDH	5’-CATGGCCTTCCGTGTTCCTA-3’	5’-CCTGCTTCACCACCTTCTTGA-3’
mβ-actin	5’-GGTCATCACTATTGGCAACG-3	5’-ACGGATGTCAACGTCACACT-3
mAip	5’-GAGGACGGGATCCAAAAGC-3	5’-CTGTGCAGCGTCCGAAAGT-3
In situ hybridization		
mPOP	5’-CCGTGCAGGAGTATCATGG-3’	5’-TTGGGGTCCAGGAACACT-3’
mFlt1	5’-CTTTCTCAAGTGCAGAGGGG-3’	5’-TCATGTGCACAAGTTTGGGT-3’
Bisulfite sequencing		
CGI-1	5’-GGTTAGGGAAGAGGTAAAGT-3’	5’-CCCCAAATACCCATACCTAC-3’
CGI-1 nested	5’-CTAAATTCAAACTAAAAAAAACCCC-3’	5’-GGTGTTTTTGTAGAGGGAGTTG-3’
CGI-2	5’-GGTTGGGTTATTTTAGGGATTTG-3’	5’-CCCCCTTTCCCCCTTTTAAA-3’
CGI-2 nested	5’-GGTAGTGTAGGTTGTTGTGG-3’	5’-CCAACCCAAAACATCAAAAACTTAC-3’
Chromatin immunoprecipitation		
mAip promoter	5’-GGGCTTCAGCACAGAATCCA-3’	5’-TGAAAAATCCTGAGAGCCTCATT-3’
mGAPDH promoter	5’-TGCTTCTGCCTGACTTCTGT-3’	5’-CGTGATGAGAAGCTGAAGGA-3’
mβ-actin promoter	5’-TGTGACGTTGACATCCGTAA-3’	5’-TGCTAGGAGCCAGAGCAGTA-3’
mPOP 5’ flanking	5’-CAGCCAAATGGCTATGTTCA-3’	5’-TGGCCAGGTAAATGGACTCT-3’
mPOP promoter	5’-TCACGATCACCTTGAAGCAT-3’	5’-AAACTTTGCCTCTTCCCTGA-3’
mPOP gene body	5’-CCATTGAGTGTTGGGAACAG-3’	5’-GGAGAGTTCACCACGTTCCT-3’
mPOP CG2	5’-TCGGATATGTTTGCGTTCAT-3’	5’-GGTTTCTTGGTCAGGATGGT-3’
mPOP 3’ flanking	5’-AAATTGGGGTGCAACCTATG-3’	5’-GCTGCTGCTTCTGTCTTCAC-3’

Table 2

Oligonucleotide primers used for RT-PCR of the neighboring genes.

Designation	Forward	Reverse
mAtg5	5’-GCTGCACACACTTGGAGATCTC-3’	5’-GAATCATCACCTGGCTCCTCTT-3’
mPrdm1	5’-CCCAAGAATGCCAACAGGAA-3’	5’-GCGCATCCAGTTGCTTTTC-3’
mPopdc3	5’-CCCCCTTTCAGTTCCTGGAT-3’	5’-GCAATCGGTGTCTGCTGTGA-3’
mBves	5’-TTGCTTTGCAGTTGGTTTGC-3’	5’-TGGCCCAGACCACATAAAGG-3’
mLin28b	5’-GGATTCGGATTCATCTCCAT-3’	5’-CCACTGGCTCTCCTTCTTTC-3’
mHace1	5’-TGCCGGAAATTGATGTAAATGA-3’	5’-TTCCACAACTTCCCAGAACCA-3’

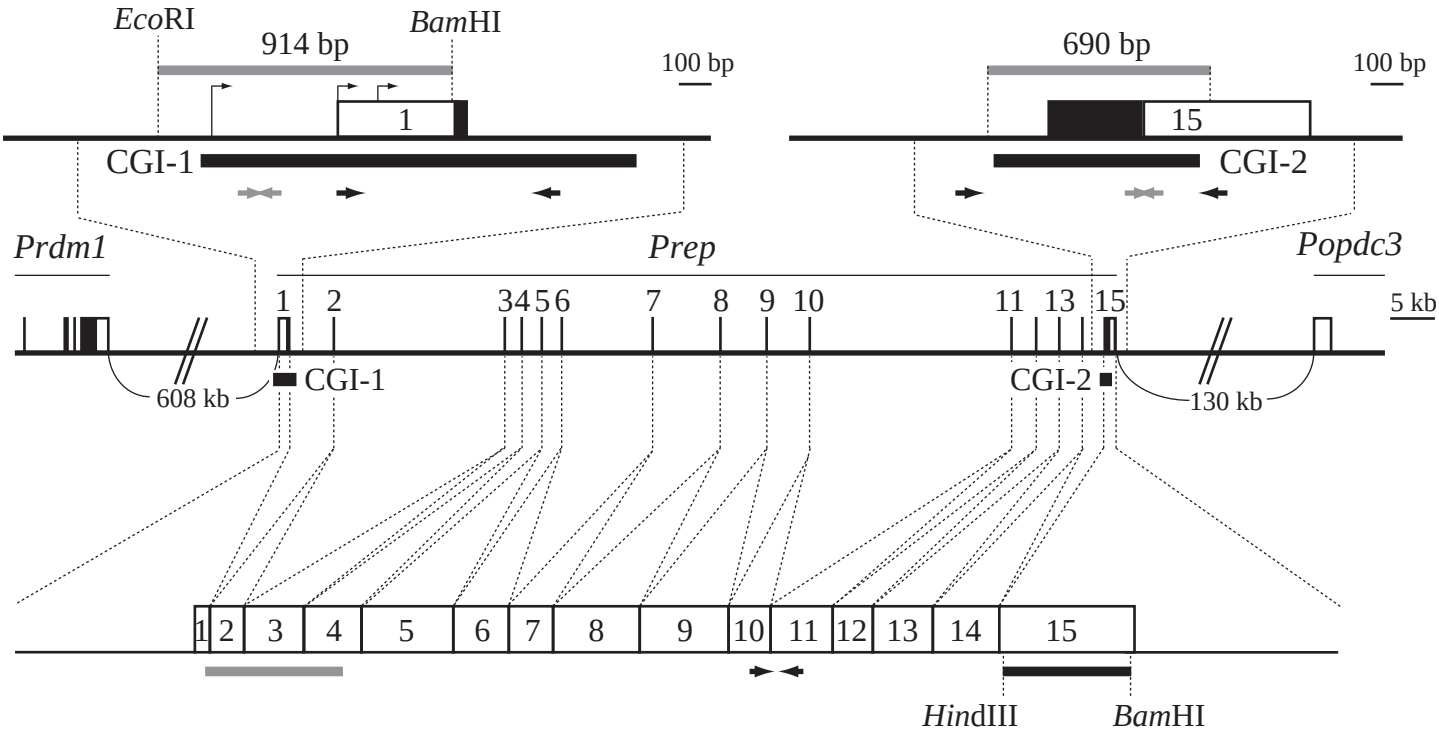
EcoRI
914 bp
BamHI
100 bp
1
CGI-1
690 bp
100 bp
15
CGI-2
Prdm1
Prep
Popdc3
1 2 3 4 5 6 7 8 9 10 11 13 15
5 kb
608 kb
CGI-1
CGI-2
130 kb
1 2 3 4 5 6 7 8 9 10 11 12 13 14 15
HindIII
BamHI

Fig.1

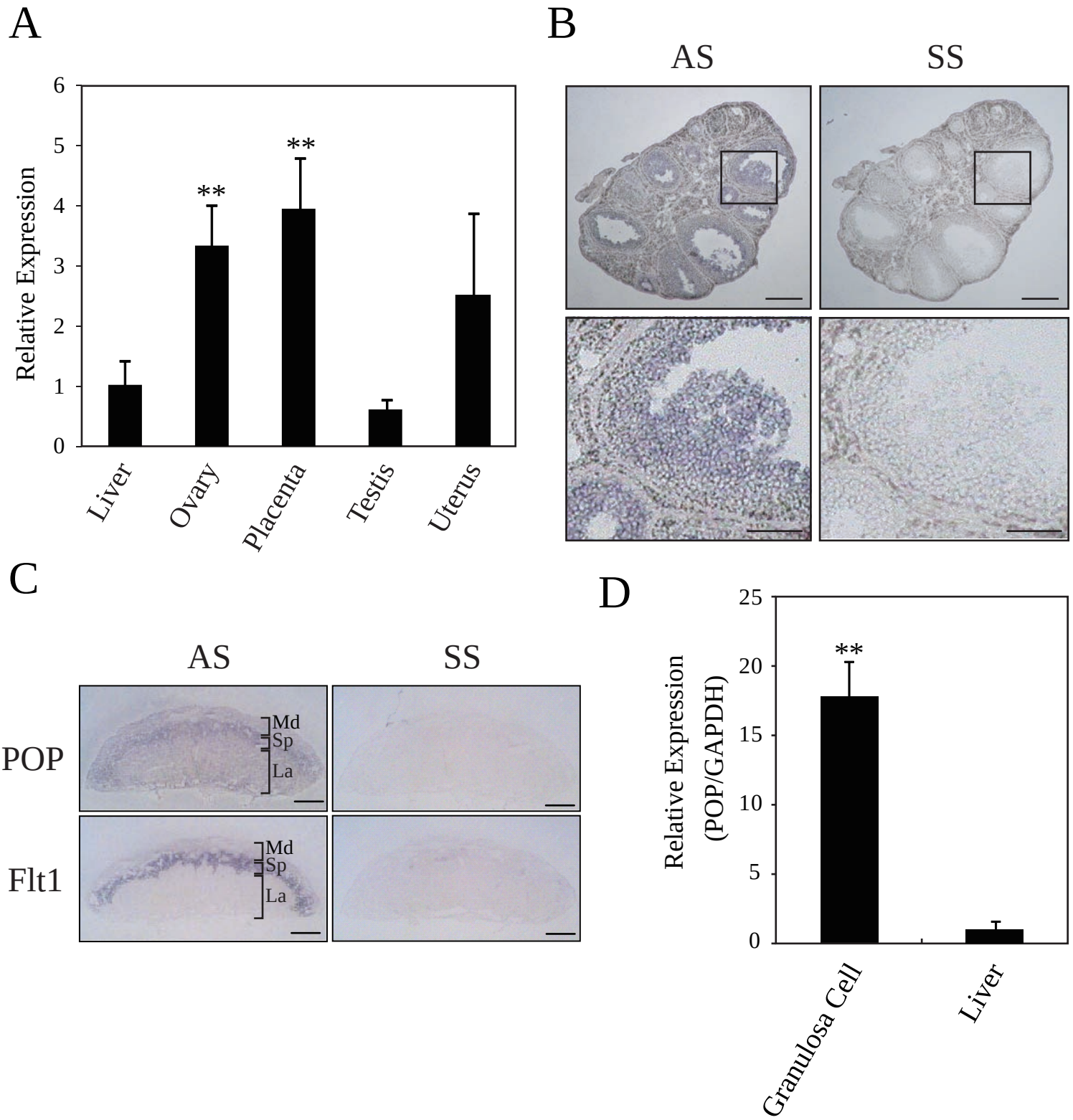
A
Relative Expression
6
5
4
3
2
1
0
**
**
Liver
Ovary
Placenta
Testis
Uterus
B
AS
SS
C
AS
SS
POP
Flt1
Md
Sp
La
Md
Sp
La
D
Relative Expression
(POP/GAPDH)
25
20
15
10
5
0
**
Granulosa Cell
Liver

Fig.2

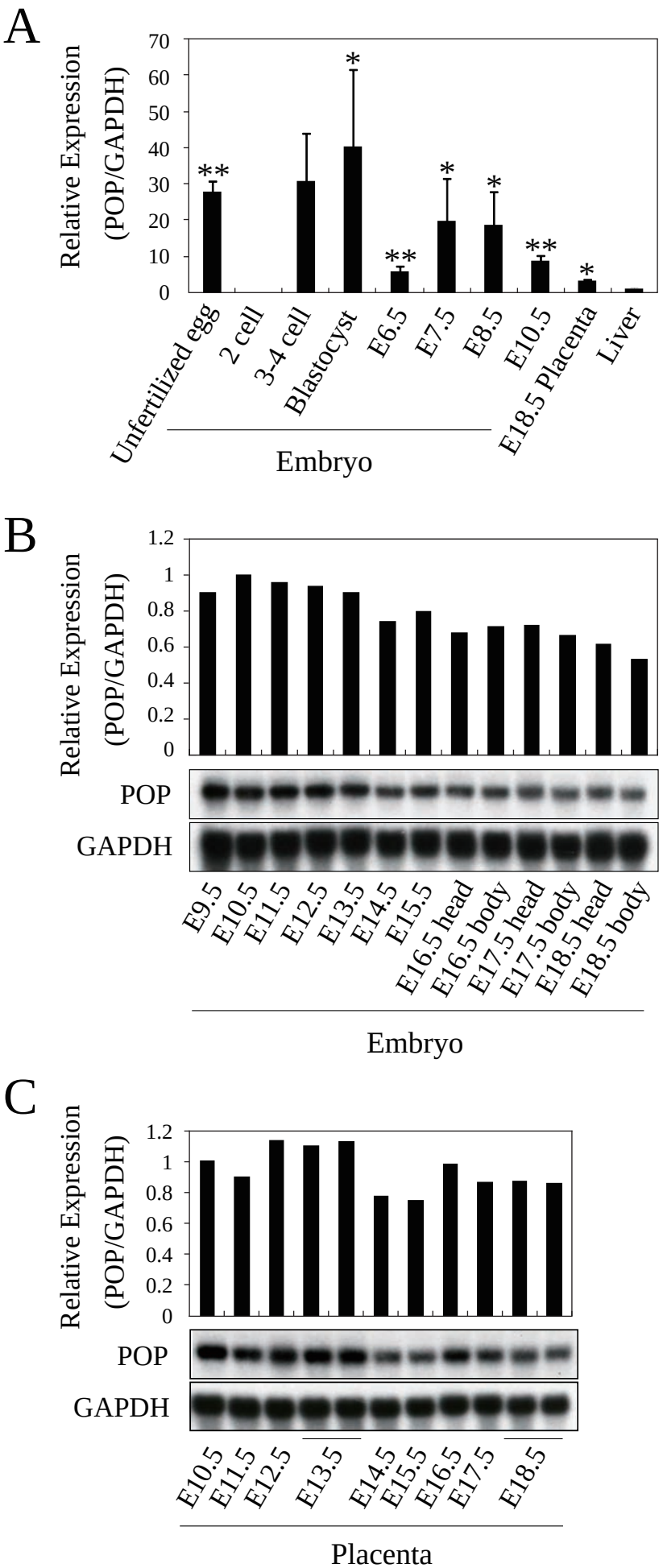
A
Relative Expression
(POP/GAPDH)
70
60
50
40
30
20
10
0
**
*
**
*
*
**
*
Unfertilized egg
2 cell
3-4 cell
Blastocyst
E6.5
E7.5
E8.5
E10.5
E18.5 Placenta
Liver
Embryo
B
Relative Expression
(POP/GAPDH)
1.2
1
0.8
0.6
0.4
0.2
0
POP
GAPDH
E9.5
E10.5
E11.5
E12.5
E13.5
E14.5
E15.5
E16.5 head
E16.5 body
E17.5 head
E17.5 body
E18.5 head
E18.5 body
Embryo
C
Relative Expression
(POP/GAPDH)
1.2
1
0.8
0.6
0.4
0.2
0
POP
GAPDH
E10.5
E11.5
E12.5
E13.5
E14.5
E15.5
E16.5
E17.5
E18.5
Placenta

Fig.3

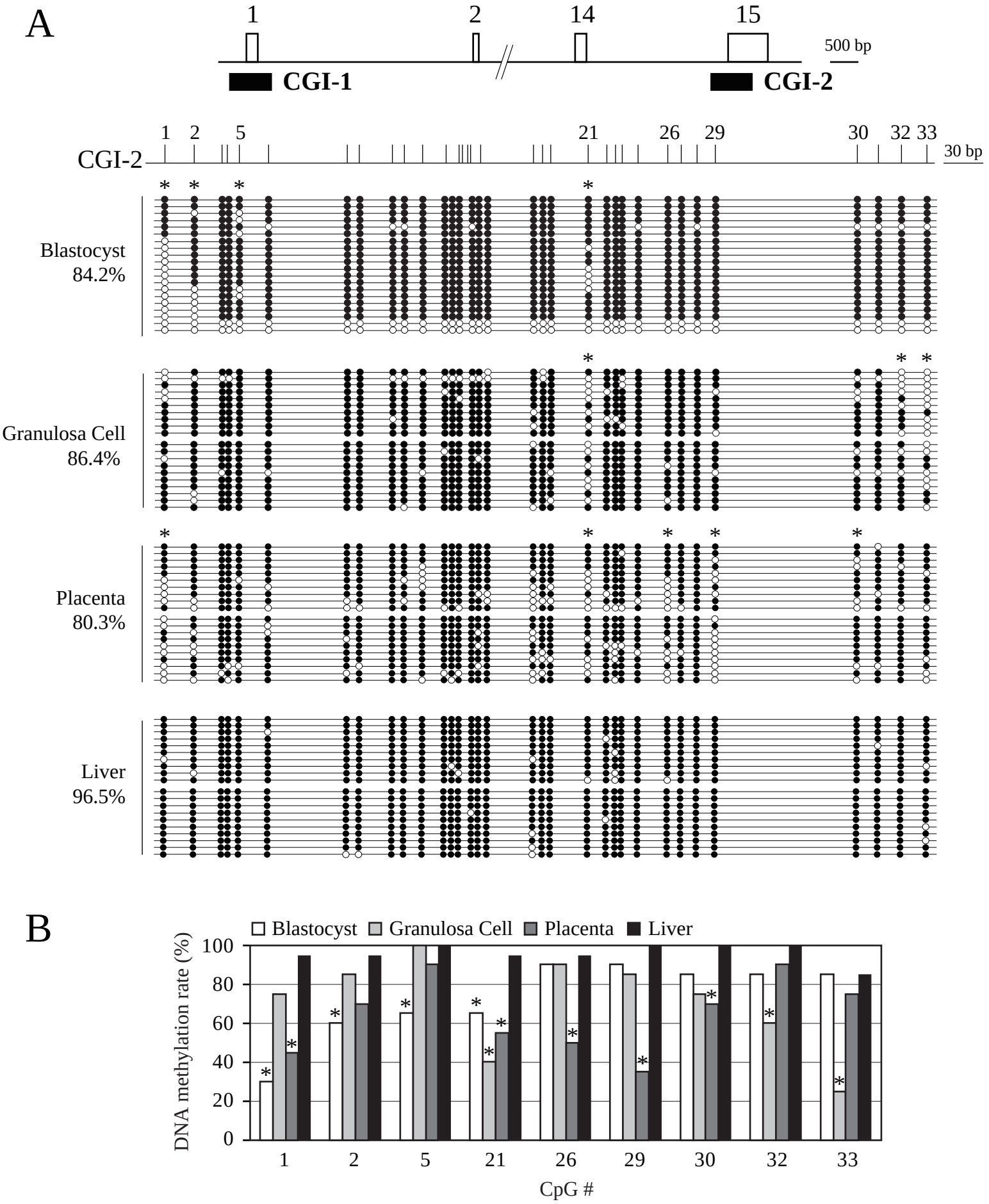
A
1
2
14
15
500 bp
CGI-1
CGI-2
1 2 5 21 26 29 30 32 33
CGI-2
30 bp
Blastocyst
84.2%
Granulosa Cell
86.4%
Placenta
80.3%
Liver
96.5%
B
Blastocyst
Granulosa Cell
Placenta
Liver
DNA methylation rate (%)
0
20
40
60
80
100
1
2
5
21
26
29
30
32
33
CpG #

Fig.4

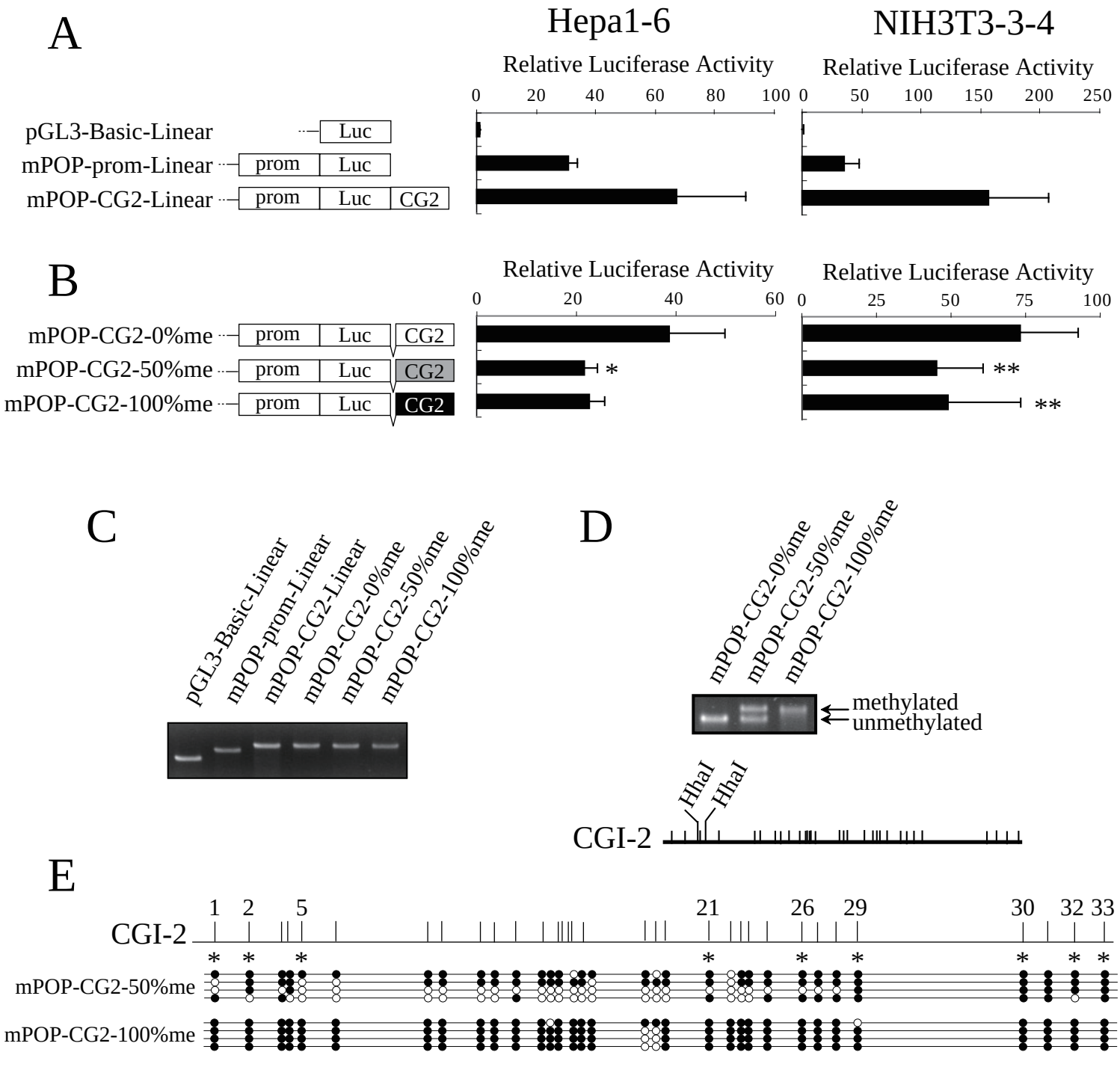
A
Hepa1-6
NIH3T3-3-4
Relative Luciferase Activity
Relative Luciferase Activity
0 20 40 60 80 100
0 50 100 150 200 250
pGL3-Basic-Linear
mPOP-prom-Linear
mPOP-CG2-Linear
Luc
prom
CG2
B
Relative Luciferase Activity
Relative Luciferase Activity
0 20 40 60
0 25 50 75 100
mPOP-CG2-0%me
mPOP-CG2-50%me
mPOP-CG2-100%me
*
**
**
C
pGL3-Basic-Linear
mPOP-prom-Linear
mPOP-CG2-Linear
mPOP-CG2-0%me
mPOP-CG2-50%me
mPOP-CG2-100%me
D
mPOP-CG2-0%me
mPOP-CG2-50%me
mPOP-CG2-100%me
methylated
unmethylated
HhaI
HhaI
CGI-2
E
CGI-2
1 2 5 21 26 29 30 32 33
mPOP-CG2-50%me
mPOP-CG2-100%me

Fig.5

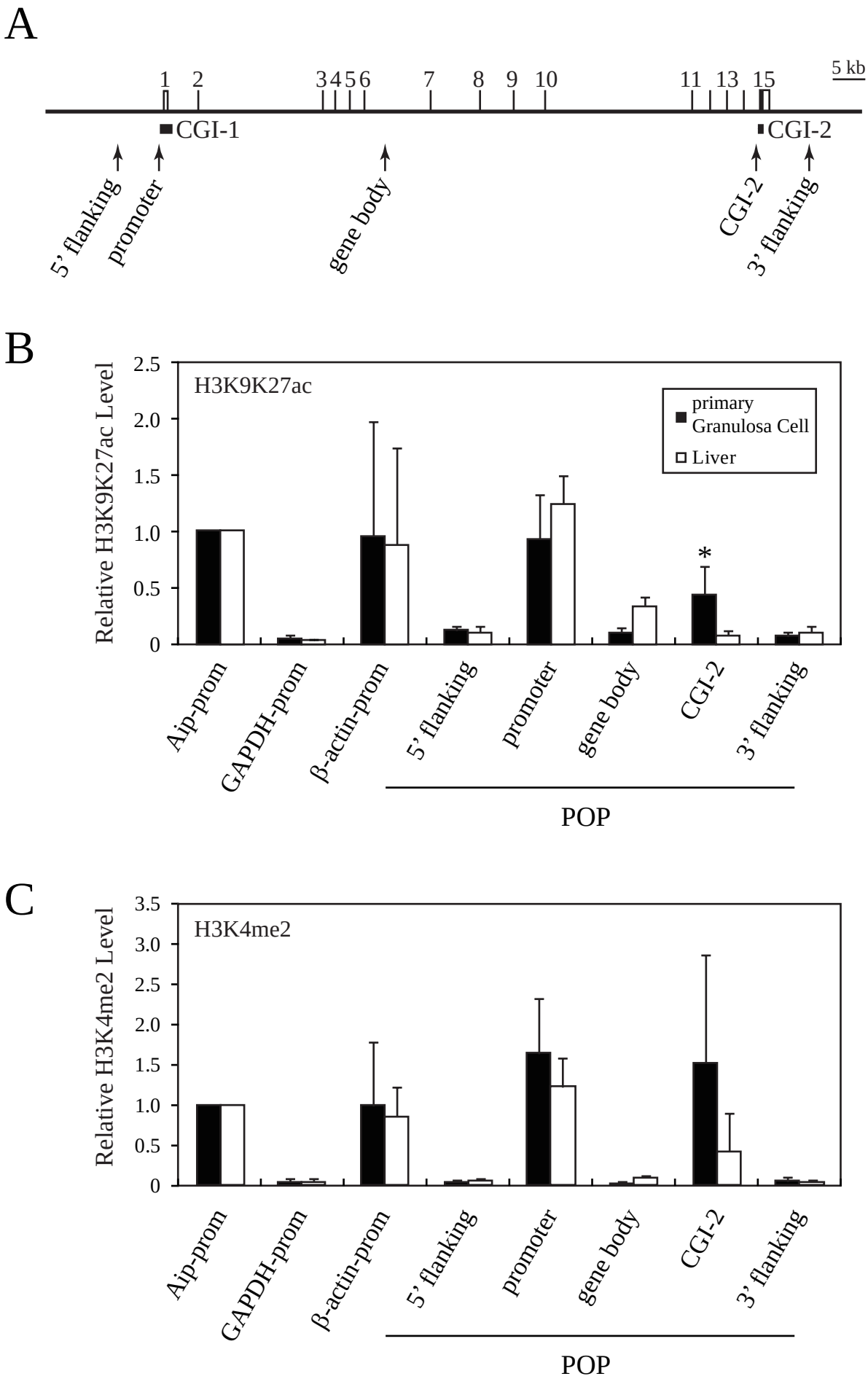
A
1 2 3 4 5 6 7 8 9 10 11 13 15
5 kb
CGI-1
CGI-2
5' flanking
promoter
gene body
CGI-2
3' flanking
B
H3K9K27ac
Relative H3K9K27ac Level
2.5
2.0
1.5
1.0
0.5
0
primary Granulosa Cell
Liver
*
Aip-prom
GAPDH-prom
β-actin-prom
5' flanking
promoter
gene body
CGI-2
3' flanking
POP
C
H3K4me2
Relative H3K4me2 Level
3.5
3.0
2.5
2.0
1.5
1.0
0.5
0
Aip-prom
GAPDH-prom
β-actin-prom
5' flanking
promoter
gene body
CGI-2
3' flanking
POP

Fig.6

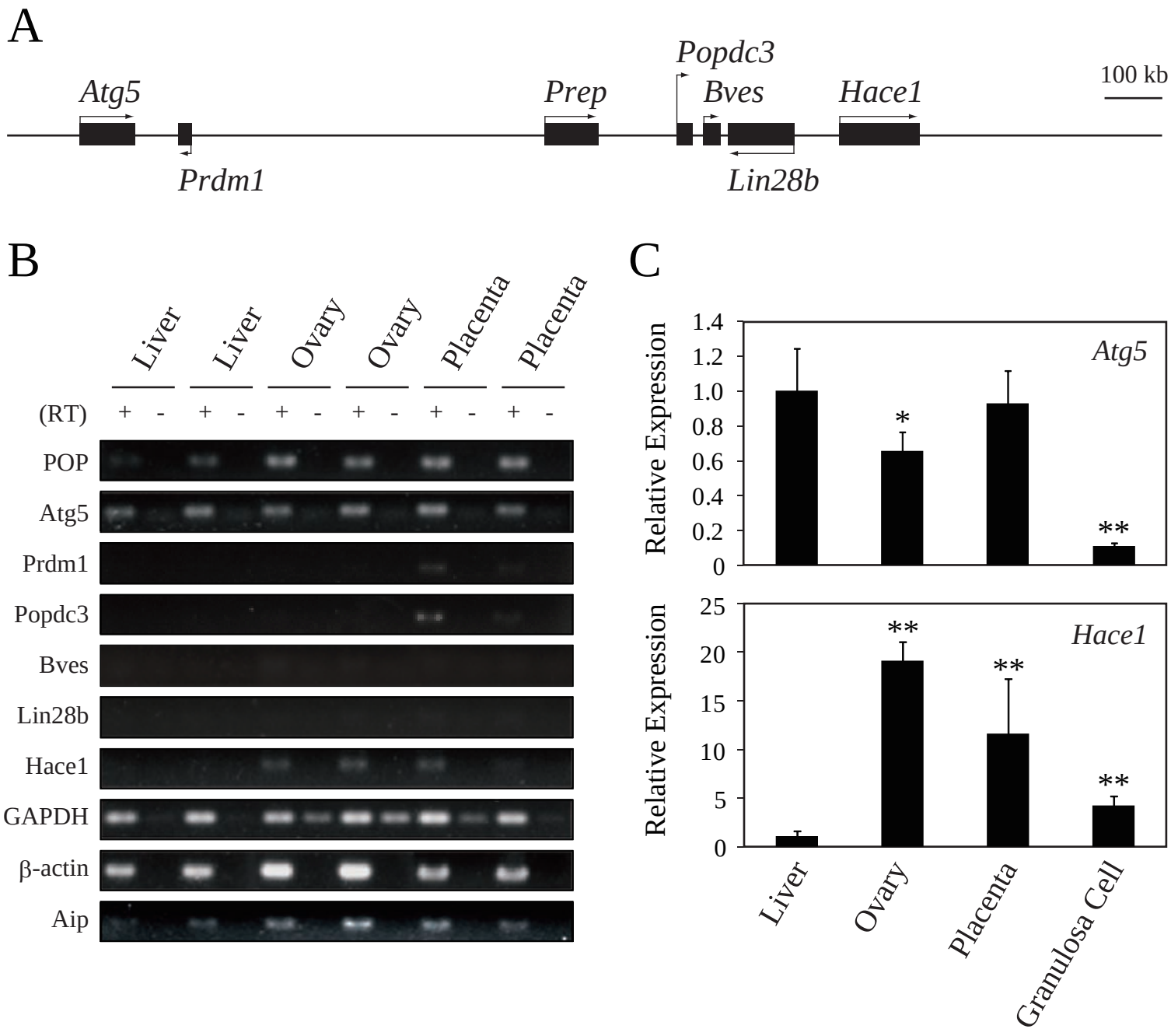
A
Atg5
Prdm1
Prep
Popdc3
Bves
Lin28b
Hace1
100 kb
B
Liver
Liver
Ovary
Ovary
Placenta
Placenta
(RT)
+ - + - + - + - + - + -
POP
Atg5
Prdm1
Popdc3
Bves
Lin28b
Hace1
GAPDH
β-actin
Aip
C
Relative Expression
Atg5
Hace1
Liver
Ovary
Placenta
Granulosa Cell

Fig.7

Supplementary Fig. 1. qRT-PCR analysis of *POP* in the liver, ovary, placenta, testis, and uterus. Total RNA was prepared from the five tissues and one microgram of the RNA was used for reverse transcription. *POP* mRNA expression was analyzed by real time PCR using the ABI Prism 7300 real-time PCR system. *POP* mRNA levels were separately normalized to *GAPDH* (black bars), *β-actin* (gray bars), and *Aip* (white bars) and relative expression is shown as -fold difference calculated relative to the expression in the liver, which was arbitrarily set at 1.0. The data are presented as mean ± SE from four independent experiments with two tissues. $n = 4$; *, $P < 0.05$ and **, $P < 0.01$ compared with liver.

Supplementary Fig. 2. (A) Comparison of *POP* mRNA in the ovarian granulosa cell and liver. Total RNA was prepared from granulosa cells which were obtained with 3 superovulated mice. Three micrograms of the RNA was used for qRT-PCR analysis. *POP* mRNA levels were normalized to *β-actin* and relative expression is shown as -fold difference calculated relative to the expression in the liver, which was arbitrarily set at 1.0. (B) *POP* mRNA expression patterns in the mouse embryo and placenta. Total RNA was isolated from the embryos at the indicated stages, E18.5 placenta, and liver and *POP* mRNA expression was analyzed by qRT-PCR as in Fig. 3A. *POP* mRNA levels were normalized to *β-actin* and relative expression is shown as -fold difference calculated relative to the expression in the liver, which was arbitrarily set at 1.0.

Supplementary Fig. 3. DNA methylation patterns of the CGI-1 region in the blastocyst, granulosa cell, placenta, and liver. Structure of the mouse *POP* gene and positions of CGI-1 and CGI-2 regions are drawn at the top. The mouse *POP* gene is about 92 kb long containing 15 exons and the first two and last two exons are depicted by open boxes with the exon number. There are two CGIs at the locus. CGI-1 is 1344 bp long and includes exon 1 and CGI-2 is 614

bp overlapping with exon 15 as indicated by filled boxes. A detailed map of the CGI-1 region and DNA methylation patterns in each tissue are shown below the gene structure. CGI-1 includes 114 CpG dinucleotides of which 97 were analyzed here. The positions of the 97 CpG dinucleotides are shown with vertical lines. The bent arrow indicates the translational initiation site. The state of individual CGIs was determined by bisulfite sequencing. Genomic DNA was purified from 14 blastocyst embryos and two 35-mm^2 dishes of granulosa cells, two E18.5 placentas and adult livers. The DNA was treated with sodium bisulfite and the CGI-1 region was amplified by PCR. For blastocyst samples, the second round of PCR was conducted with nested primers and thereby 65 CpG dinucleotides were analyzed. Ten subclones of the amplified product for each granulosa cell, E18.5 placenta, and adult liver, and twenty for the blastocyst were analyzed by DNA sequencing. Open and filled circles represent unmethylated and methylated cytocines, respectively. The overall methylation rate for each tissue is indicated at the left.

Supplementary Fig. 4. qRT-PCR analysis of the *Atg5* (A) and *Hace1* (B) genes in the liver, ovary, placenta, and granulosa cell. Total RNA was prepared from the five tissues or two wells of granulosa cells in a 24-well plate. One microgram of the RNA was used for reverse transcription and real time PCR was performed as in Supplementary Fig. 1. The mRNA level was normalized and relative expression is shown as in Supplementary Fig. 1. The data are presented as mean ± SD from four independent experiments. $n = 4$; *, $P < 0.05$ and **, $P < 0.01$ compared with liver.

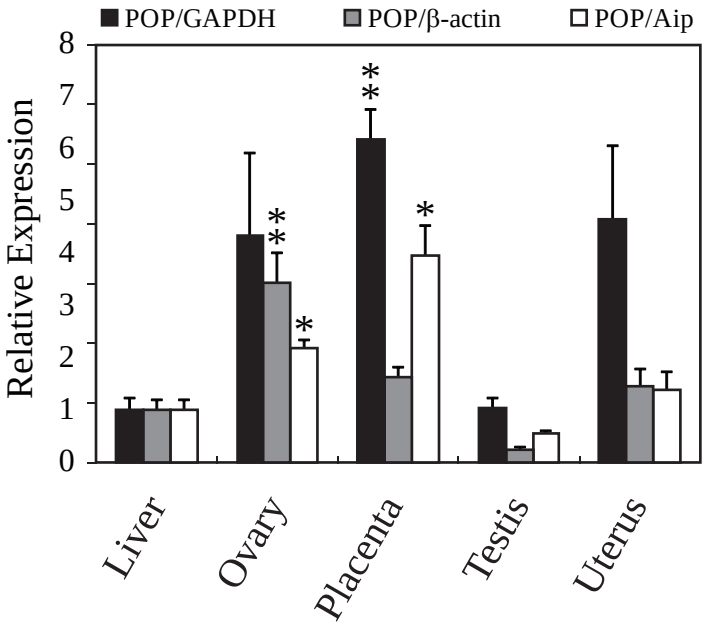

Supplementary Fig.1

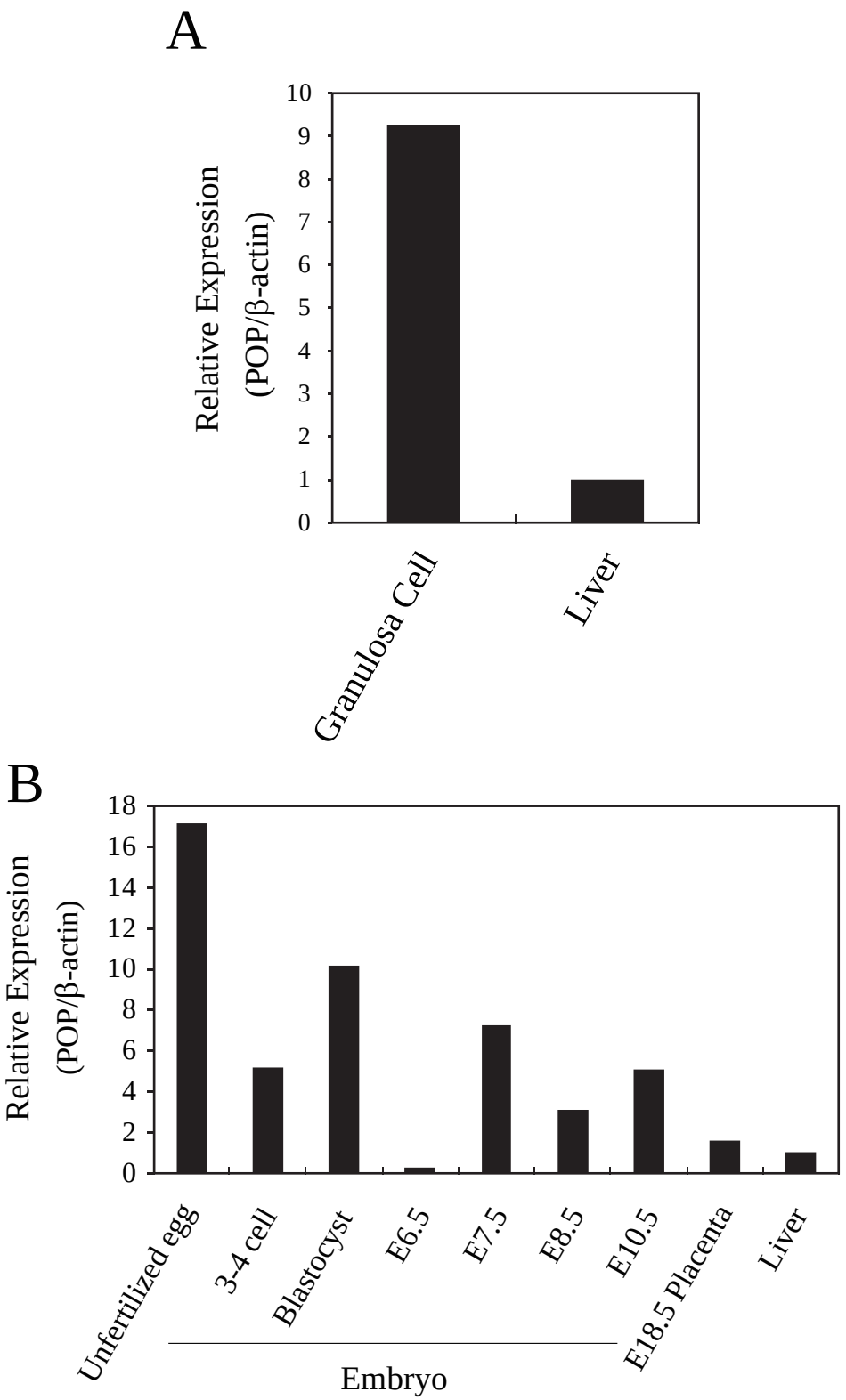

Supplementary Fig.2

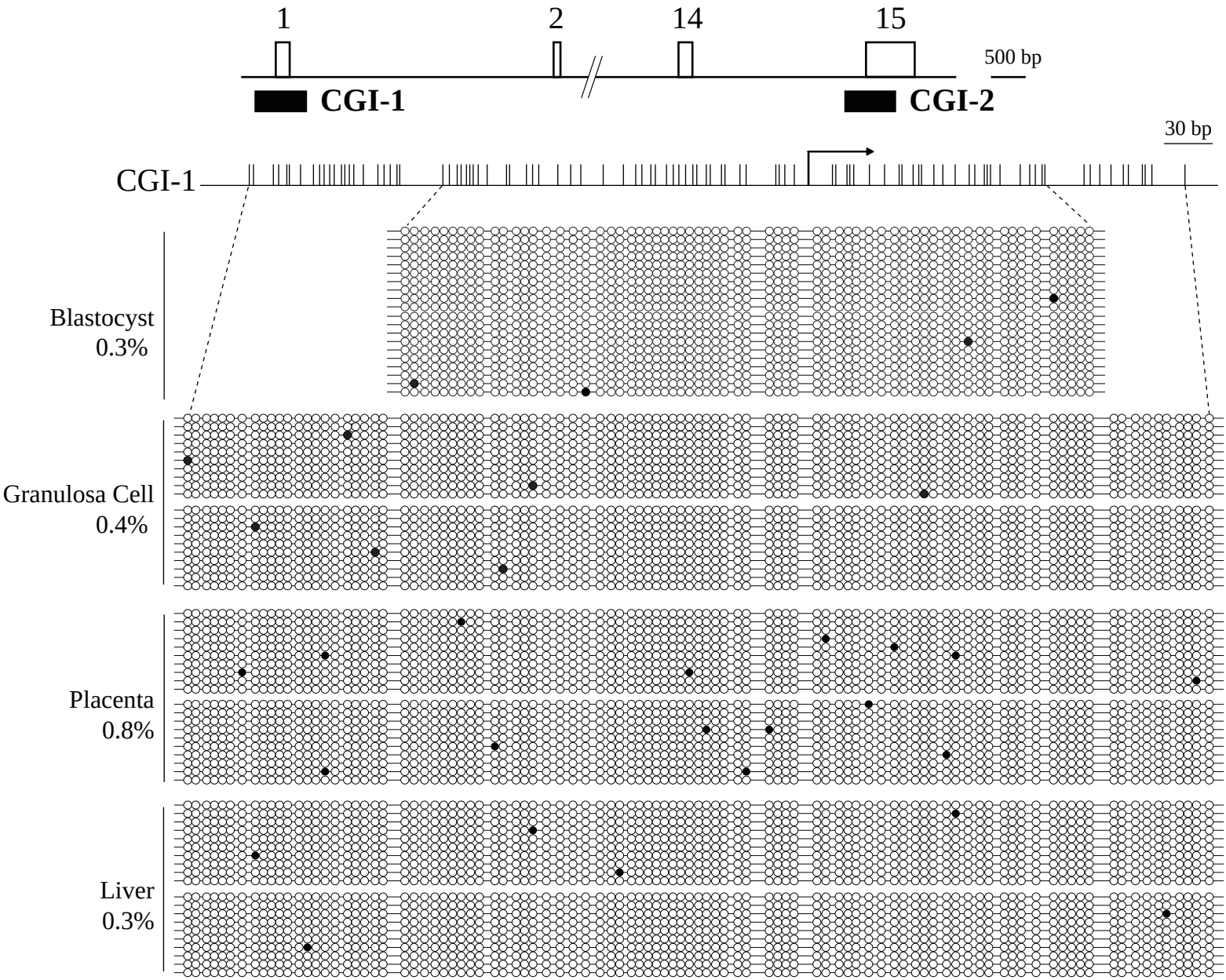

Supplementary Fig.3

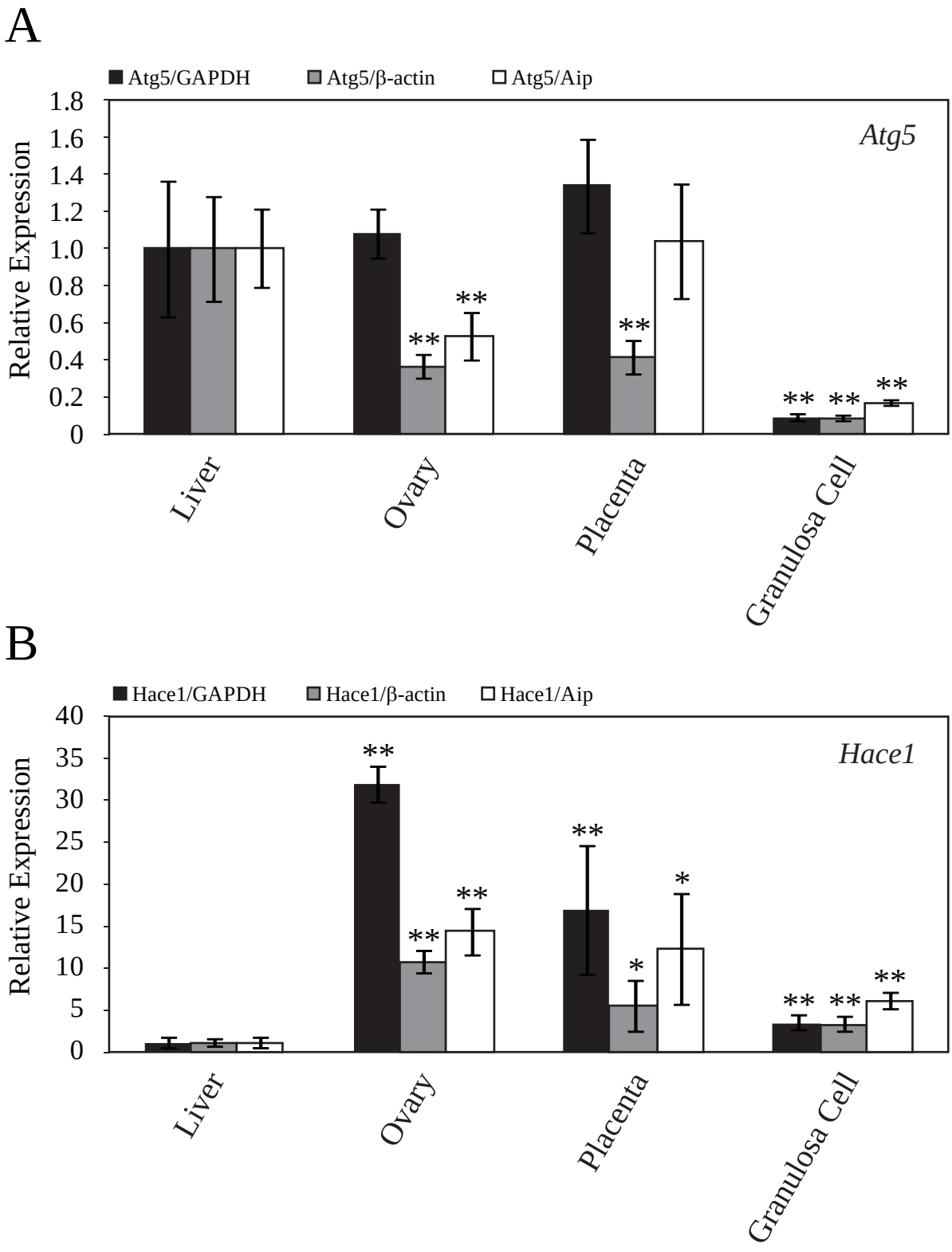

Supplementary Fig.4